# THE PLASTIC DEFORMATION PROCESS OF METALS – 50 YEARS DEVELOPMENT OF A DISLOCATION BASED THEORY

## *"A journey from homogeneous to inhomogeneous plastic deformation"*

Yngve Bergström

## INTRODUCTORY SUMMARY

The Bergström dislocation model for homogeneous plastic deformation of pure single phase metals has been gradually developed over the years. We begin with a brief review of the various steps taken in this development process.

About 6 years ago a more thorough further-development of the theory was initiated in order to include also inhomogeneous plastic deformation which, inter alia, occurs in metals composed of hard and soft phases – e.g. modern, advanced high-strength metals such as dual-phase (DP) steels and LTT Martensitic steels but also high-strength fcc metals containing µm-sized hard particles.

Based on this further – development, it has been possible, firstly, to improve the physical basis of the theory and, secondly to improve its ability to describe the uniaxial true stress – true strain behavior of various types of inhomogeneous metals. This is made possible by a transformation of the global strains obtained in uniaxial tensile testing, $\varepsilon_g$, to the actual local average strains, $\varepsilon_l$, which occurs in a strain dependent local fraction, f(ε), of the test-sample volume. For single phase pure metals it holds that $\varepsilon_l \sim \varepsilon_g$, while $\varepsilon l >> \varepsilon g$ for advanced high strength metals.

For an investigated single-phase ferritic steel, $\varepsilon_l \sim 14$ % and $\varepsilon_g \sim 12.5$ % which may be regarded as a minor local inhomogeneity effect, presumably caused by varying resolved shear stresses in the slip planes due to varying directions of the grains. Hence, some shear stresses will exceed the critical shear stress and cause local plastic deformation. There might also be smaller effects caused by the release of residual stresses and stress concentrations causing locally distributed bursts of dislocation generation.

For a DP800 steel, $\varepsilon_l \sim 12\%$ while $\varepsilon_g \sim 6\%$ which represents a rather strong inhomogeneity effect. In the extreme case of a LTT 1700M martensitic steel $\varepsilon_l \sim 55\%$ while $\varepsilon_g \sim 2.5\%$. These powerful local strain- and strain hardening effects are the main causes of the excellent combinations of the high strength and the good ductility characteristics of the latter types of metals.

The basic reason for the differences in the global and local strain values, evaluated from a tensile test, is that it is assumed, in accordance with the standard procedure for these tests, that the entire volume of the specimen takes part in the plastic deformation process. In reality, however, only a minor fraction, f(ε), of the total volume of the tensile test specimen is participating, at least in the case of severely inhomogeneous metals. In the case of the DP800 steel the analysis indicate that the initial volume fraction, $f_1$, taking active part is approximately equal to 15%. This value then increases with strain up to a value $f_0$ approximately equal to 73%. This means that the martensite content is equal to $1\text{-}f_0 = 27\%$ which agrees well with the experimentally estimated martensite content. (According to experiments the martensite did not, in the actual cases, take active part in the plastic deformation process).

In the case of the martensitic steel LTT – 1700M it is observed that the initial volume fraction, $f_1$, taking active part in the plastic deformation process, is ~ 0.2% while the final active volume fraction is 5%. The mechanisms behind these extremely small values will be discussed in detail in a later section.

Below, we will also give a detailed presentation of the new extended dislocation model for inhomogeneous plastic deformation. We will also, on the basis of this model, present an extended analysis of the following metals:

- single phase ferritic steel, A4
- single phase Al – 0.0052Ti
- DP800 steel
- LTT-1700M martensitic steel
- Al-based AA3003 containing hard particles
- Austenitic stainless steel

Now, by analyzing pure single-phase metals as well as those containing a mixture of soft and hard phases, we obtain details of the following physical parameters, all of which are operational in the local volume fraction, $f(\varepsilon)$:

- rate constant of dislocation remobilization, $\Omega$
- the grown-in dislocation density, $\rho_0$
- initial active volume fraction, $f_1$
- final active volume fraction, $f_0$
- the corresponding rate constant, r
- initial mean free path of dislocation motion, $s_1$
- final mean free path of dislocation motion, $s_0$
- the corresponding rate constant, k
- the athermal friction stress, $\sigma_g$
- the thermal friction stress, $\sigma^*(\varepsilon)$, and its strain dependence

By knowing how these parameters vary with external as well as internal factors, it becomes possible to optimize the properties of different materials for different product applications. In the case of DP steels it has been found that said parameter values are intimately linked to the martensite content, $f_m$, and strain rate. Similar observations have been made in the studies of martensitic steel. This type of results will be discussed in coming papers.

# INTRODUCTION

## A short re-view of plastic deformation

Because plastic forming of metals and alloys is of high economic and technological importance, it is not surprising that the plastic deformation process has been the subject of extensive and basic experimental and theoretical studies over the years (1-16). The rapid development of the atomic theory at the end of the 1800s and in the early 1900s had a positive impact on the basic understanding of the atoms and of the formation of crystalline structures. It was also soon realized that it was atomic bonding that gave rise to the formation of crystals and that the elastic phenomenon was due to this bonding. It also became evident that plastic deformation occurred in certain densely packed slip planes and slip directions, see Fig. 1. Examples of individual slip bands and slip planes as well as grain boundaries in polycrystalline metals are shown in Fig. 2a. In due course it was agreed upon a hypothesis saying that elastic deformation is caused by elastic tension (not breaking) of the atomic bonds. Hence, an elastically deformed specimen retains its original shape after unloading. In the case of plastic deformation it was assumed that this occurred in certain slip planes and was caused by the fracture of atomic bonds. Hence, the change in shape remains after unloading.

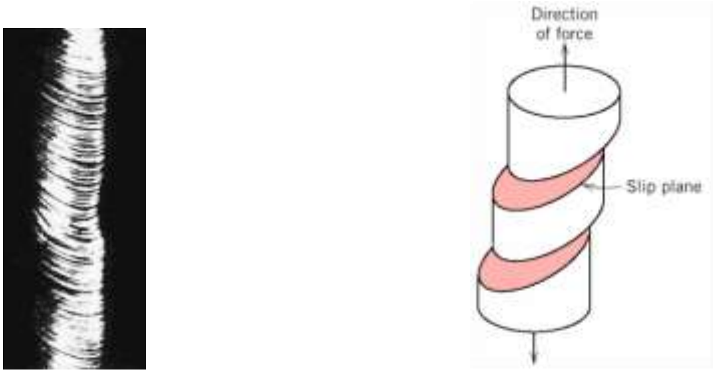

(a) (b)

***Fig.1. a/ shows a single crystalline Zn – crystal that has been subjected to vertical uniaxial tension. We can see that the plastic deformation has occurred along a certain type of slip planes. This is schematically illustrated in (b). This type of movement is similar to the movement of cards in a deck of cards. (University of Tennessee, Dept. of Materials Science and Engineering: Dislocations and Strengthening Mechanisms - Chapter 7).***

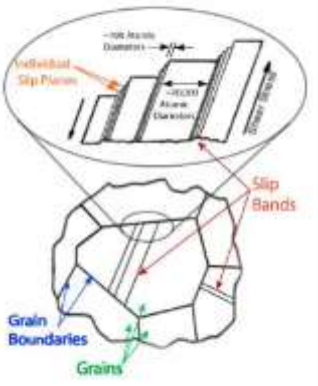

***Fig.2a. Grains, grain boundaries, slip planes and slip bands in a crystal. The orientation of the grains is random with respect to the applied stress. The dislocations are moving along slip systems with preferable orientation. (Wikipedia)***

***A comparison between the shear strengths in some metals***

| **Material** | **Theor. hardn. MPa** | **Exp. hardn. MPa** | $\tau_{theor}/\tau_{exp}$ |
|---|---|---|---|
| **Copper** | **19600** | **0,49** | **~ 40000** |
| **Silver** | **12600** | **0,37** | **~ 34000** |
| **Magnesium** | **7000** | **0,39** | **~ 18000** |
| **Aluminium** | **11300** | **0,78** | **~ 14500** |
| **Iron** | **33900** | **27,5** | **~ 1200** |
| **Titanium** | **16900** | **13,7** | **~ 1200** |
| **Molybdenum** | **54100** | **71,6** | **~ 760** |
| **Niobium** | **16600** | **33,3** | **~ 500** |

***Fig. 2b.Theoretical and experimental shear strength – a comparison (Wikipedia)***

It was initially assumed that all atomic bonds in a slip plane must break simultaneously for glide to occur. However, a comparison between experimental, $\tau_{exp}$, and theoretical, $\tau_{theor}$, shear strengths showed that the quotient $\tau_{theor}/\tau_{exp}$ attained values in the range 40 000 to 500 dependent on metal, see Fig. 2b. It was then easily realized that the latter type of assumption was wrong and that new ideas were required.

The work continued and in 1907 Volterra (17), see Fig. 3a, solved the problem by introducing the concept of dislocations, see Fig 3b. This ingenious idea by Volterra has made it possible to steadily improve the knowledge of the plastic deformation process of metals. However, lots of work remains to be done, and the potential for further improvements of the properties of materials to better suit various types of different applications, is large.

*Fig. 3a. Vito Volterra –Father of the dislocation theory – 1907 (Wikipedia)*

The dislocation is a linear local defect which in a crystal carries a small shearing step, b, when it moves along a slip plane. The step b is the magnitude of the Burgers vector. When the dislocation has moved across the entire shear plane the upper plane has moved the distance b relatively the lower one, see Fig. 3b. Since the distance b is small – ca 2.5 Å – large numbers of dislocations are required to explain large plastic deformations. Dislocation density measurements of heavily deformed metals indicate density values in the range $5 \cdot 10^{14}$ - $5 \cdot 10^{17}$ $m^{-2}$, dependent on type of metal and amount of deformation (14).

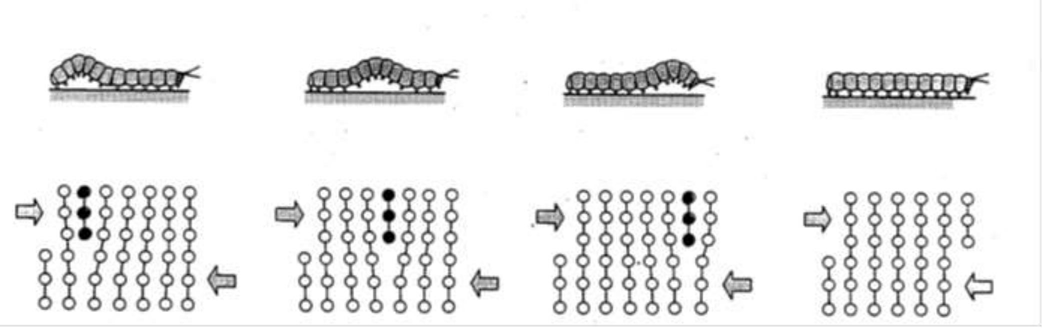

*Fig. 3b Shear – one step – via an edge dislocation moving in a slip plane (Wikipedia)*

Volterras (17) idea that the plastic deformation process is inhomogeneous and connected to dislocations in motion has proved to be pioneering and has opened the doors for an increased physical understanding of the complicated plastic deformation process of metals.

History shows over and over again that it is the art of “seeing the simplicity in the behavior of nature” that is the real difficulty. Isaac Newton`s (8) assumption that there is a gravitational force between bodies and the Alfred Wegener`s (19) hypothesis that the earth crust consists of so-called tectonic plates that move relative to each other, are further examples of just such innovative successful ideas and stories.

It is said that Albert Einstein was once asked by a worried mother what literature he thought that her son ought to study to quickly get started with his scientific work. The answer she got was the following: “tell him to read fairy tales and teach him how to dream”.

> Hence, we must be able to see past, and rid us from the various types of established beliefs that constantly surround us. They are like sticky spider webs in which we easily get stuck, thus hampering our ability for innovative thinking.

Or might it be that Volterra (17) perhaps was inspired to his dislocation idea by the Lϋders bands observed in e. g, single-phase ferritic steel in the initial stages of uniaxial tension, see Fig. 4. In such cases, the plastic deformation is located at the front of macroscopic bands, slowly moving along the sample at a fairly constant stress. The corresponding strain is called the Lϋders strain.

The local strain in the band fronts is, however, several percent, and thus much larger than the mini deformation carried by a dislocation. It also holds that the Lϋders band penetrates the whole thickness of the specimen while a dislocation moves in well-defined slip planes inside the specimen, see Fig. 4.

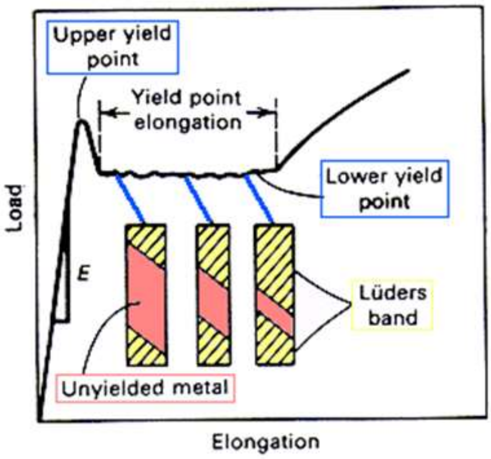

*Fig. 4 Propagation of Lϋders bands during uniaxial tension. (Wikipedia)*

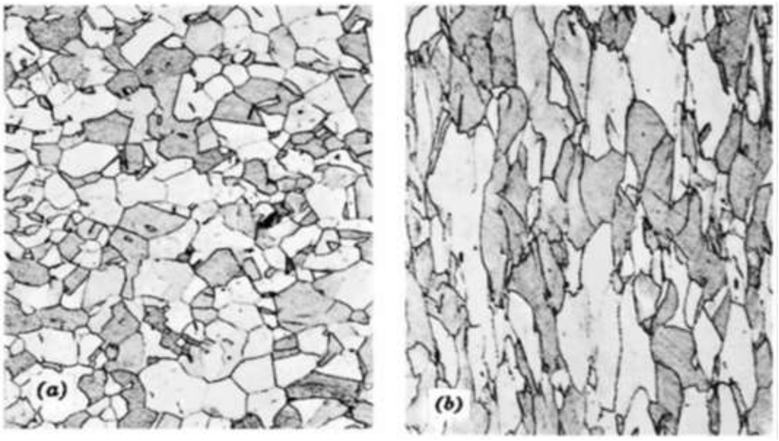

**before deformation** **after deformation**

*Fig.5. Change in the shape of the grains as a result of a large plastic deformation (vertical loading).University of Tennessee, Dept. of Materials Science and Engineering: Dislocations and Strengthening Mechanisms - Chapter 7*

It is interesting to note, however, that both these phenomena - dislocations and Lϋders bands - are closely related to one another through their local character. We may therefore, already at this stage, conclude that the plastic deformation is essentially inhomogeneous. The question, however, is what the underlying mechanisms may look like, how extensive the inhomogeneity is and how this physically affects the deformation process in its entirety. These are important questions that we, inter alia, will touch on in this article.

An example of how large plastic deformations elongate the grains in the direction of the applied tensile stress in a polycrystalline material is shown in Fig. 5

We also know through comprehensive TEM studies that dislocations are generated, moving and becoming immobilized as a result of plastic deformation. They may also interact with each other and with different types of other defects which are present in crystalline materials. The dislocation substructures resulting from this interaction include: dense clusters of dislocations - so-called tangles - and dislocation cell structures (14, 16, 20).

Dislocations may also annihilate or remobilize which leads to so-called dynamic recovery (14, 20).

The development in the area of plastic deformation has progressed in steps, and has been promoted by the emergence and development of various experimental techniques, such as X-ray, transmission electron microscopy, scanning electron microscopy, various mechanical testing techniques, computer analysis techniques, and so on. The basic knowledge about the plastic deformation process has thus gradually increased and new theories that have been developed. Simultaneously, other theories have been revised, refined or thrown in the trash.

## Uniaxial tensile testing as well as global and local strains

The uniaxial tensile test is one of the most frequently used methods to document, test and analyze the mechanical properties of metallic materials. A uniaxial stress state also makes it easier to test theoretical models and to analyze how the effects of different structure parameters and other physical parameters influence the plastic deformation process.

Now, if we want to use experimental stress-strain data recorded by conventional standard uniaxial tests in order to analyze the stress-strain behavior of inhomogeneous materials we must find a method to transform the global strain, $\varepsilon_g$, to the local strain, $\varepsilon_l$, see above. The reason is that it is assumed, in the uniaxial tensile test standard, that the total specimen volume takes active part in the plastic deformation process and that this volume is hence strain independent.

Since only a strain dependent fraction, f(ε), of the test specimen volume takes part in the plastic deformation process of inhomogeneous materials, the only reasonable physical conclusion is that $\varepsilon_l$ is larger than the global strain $\varepsilon_g$. We will in the theory section show that, f(ε), can in fact be used to transform $\varepsilon_g$-values to $\varepsilon_l$-values.

For details regarding the uniaxial tensile test, see Appendix 1.

## Macroscopic inhomogeneity

As an example of how theories may follow the general trend of knowledge-growth in the field, we shall recapitulate how the Bergström original dislocation model of plastic deformation of metals ( 13, 14) in different steps, has been further developed since its inception in the mid -1960s and up to date.

To-day the theory also includes inhomogeneous materials and we shall in some detail, present this expanded theory and its applicability to describe the work hardening behavior of advanced high strength steels and other hard-phase strengthened metals, for instance aluminum.

Of special interest in this particular context is the great effect the *inhomogeneity* has on the plastic deformation process of polycrystalline metallic materials. If a material is built up of hard and soft phases, e.g. ferrite and martensite, being the basic phases of a DP steels, it is reasonable to assume that the soft phase is the one that first starts to deform plastically. Now, since the soft ferrite phase represents only a fraction of the specimen volume, it is easily realized that the plastic deformation becomes inhomogeneous, yes it becomes *macroscopically inhomogeneous*. We will also show that the ferrite phase deforms inhomogeneously , which in turn further enhances the inhomogeneity effect as well as the local rate of dislocation generation. The combined result of these effects is an increased deformation hardening and an increased ductility potential. Experiments indicate that the corresponding martensite is deformed only slightly, or not at all, for strains up to necking.

It seems that this macroscopic effect has mostly been ignored in the theories presented in the literature so far. Instead focus has been directed towards micro- and sub micro inhomogenities.

## Content

It is the objective of this presentation therefore to show that macroscopic inhomogeneity has a dominant impact on, inter alia, the increased strain hardening and the related improved ductility of high strength metallic materials. Similar positive effects are also observed in aluminum and other FCC materials containing hard particles or hard phases. We shall furthermore also consider the impact that other types of structural defects can have on the deformation process.

To get an overall picture of developments in the actual field we shall in the present compilation also briefly discuss the elastic deformation process including Hookes law (21) as well as Ludwik and Hollomon (22) empirical equations for plastic deformation. We shall also describe Taylors (15) groundbreaking equation for the relationship between the plastic flow stresses, $\sigma$ ($\varepsilon$), and $\sqrt{\rho(\varepsilon)}$ where $\rho(\varepsilon)$ is the total dislocation density.

We will therefore, in turn, address the following points:

- Hookes law (21) for elastic deformation
- Ludwik and Hollomon empiric relationships for uniaxial plastic deformation
- Taylor´s equation (15) for the relationship between flow stress and the square root of the total dislocation density.
- Taylor´s strain hardening theory (15) for homogeneous metals
- Bergströms initial theories (14) for homogeneous plastic deformation (14) – Step 1 and Step 2
- The presence of various defects in metals and their impact on the plastic deformation process
- Further development of the Bergströms original theory to include inhomogeneous plastic deformation – Step 3
- Examples illustrating how the Bergström theory for inhomogeneous plastic deformation is capable of describing the uniaxial true stress – true strain behavior of ferritic single phase steel, DP-steel, LTT-Martensitic steel, Al-bas/AA3003, pure Al and austenitic steel
- New development trends
- Conclusions

## SIMPLE EMPIRICAL AND THEORETICAL RELATIONSHIPS TO DESCRIBE UNIAXIAL ELASTIC AND PLASTIC STRESS-STRAIN BEHAVIORS OF METALS ASSUMING HOMOGENEOUS PLASTIC DEFORMATION

### Hooke´s law

The elastic stress - strain behavior of metals is linear and follows Hooke´s law (21)

$$\sigma = E \cdot \varepsilon \qquad (1)$$

Here σ is the applied stress, ε is the strain and E is the elastic modulus. This equation applies to small strains where no plastic deformation is supposed to takes place. Robert Hooke (21) published this discovery in 1678.

Since most commercial metals contain tensile residual stresses as well as various other types of local stress concentrations, an applied uniaxial tensile stress may trigger plasticity at lower stresses than the yield stress and give rise to a deviation from the linearity.

Also texture as well as mixtures of different phases may affect the results.

When the applied stress reaches a certain critical value, which is material dependent - the so-called Yield Stress - the material starts to deform plastically. Due to, for instance, the above mentioned inhomogeneity effects, the yield stress is normally defined as, $\sigma_{0.2}$, at the plastic strain of 0.2% (not at 0% strain) which to some extent eliminates the initial scatter in the stress data caused by the release of built-in local stresses.

## The Hollomon and Ludwik equations

In 1909, 231 years later than Hooke´s presentation of his equation for elastic behavior; Ludwik (23) proposed the following expression to describe the plastic stress-strain behavior of metals

$$\sigma = \sigma_0 + L \cdot \varepsilon^q \qquad (2)$$

Here σ is the true stress, ε is the true strain, $\sigma_0$, is a type of friction stress and L and q are material constants.

The following simplified version of eqn. (2) was proposed in 1945 by Hollomon (22) where K and n are material constants

$$\sigma = K \cdot \varepsilon^n \qquad (3)$$

Since eqns. (2) and (3) hold for plastic strains, the elastic strain contributions must be eliminated before the plastic stress-strain behaviors can be analyzed. Such a correction is especially important in the case of high strength materials where the elastic strains are comparatively large to the plastic strains.

The Hollomon eq. (3) has become the most widely used of all empirical equations in the material-producing as well as in the engineering industries. This equation is also frequently used in research.

A possible explanation to the popularity of this equation is presumably the fact that it is assumed that a plot of log (σ) versus log (ε) results in a straight line with slope n. Since n is assumed to be approximately equal to the strain to necking, $\varepsilon_n$, the procedure then also involves a simple way to estimate the stretch formability of a metal. There is, however, a problem, since the resulting curve rarely exhibits a linear progression since n is in fact highly strain dependent. One therefore normally observes a so-called double-n or a triple-n behavior which significantly complicates the picture (14).

In the current situation, with access to modern computers, it would maybe be better to start from a slightly more advanced empirical relationship which with greater accuracy describes the σ - ε course and then exploit the relationship dσ / dε = σ to calculate the strain to necking. The fact that the development has not gone in such a direction is obviously surprising because the technique of using log-log graphs is long since passé.

The example, however, indicates the conservatism and fear of change that sometimes can be discerned in the materials and engineering technology fields.

Several more empirical stress–strain relationships have of course been presented through the years. However, they are usually of less interest and we have therefore limited ourselves to the two ones presented above.

## The Taylor equation

Some thirty years after Volterras (17) presentation of his dislocation theory, Taylor (15) showed that this theory also could be used to explain why metals harden during plastic deformation. The reason is simply that dislocations surround themselves with stress fields that interact with each other. As the dislocation density increases with increasing plastic strain, also the stress required for dislocations to be generated and to move along the slip planes increases. This type of reasoning finally gave birth to the Taylor equation (15)

$$\sigma(\varepsilon) = \sigma_{i0} + \alpha \cdot G \cdot b \cdot \sqrt{\rho(\varepsilon)} = \sigma_{i0} + \sigma_d(\varepsilon) \tag{4a}$$

Where $\sigma(\varepsilon)$ is the true flow stress, $\varepsilon$ is the true strain, $\sigma_{i0}$, is a friction stress, $\alpha$ is a hardening parameter, G is the shear modulus an b is the magnitude of the Burgers vector. The parameter $\alpha$ can in turn be written

$$\alpha = \alpha' \cdot m \tag{4b}$$

Here $\alpha'$ is a material dependent dislocation hardening parameter with values in the interval ~ 0.1 – 0.3 and m is the Taylor factor (15) with the values ~ 2 and ~ 3.1 for polycrystalline bcc- and fcc-structures respectively.

In a bcc-structure the friction stress, $\sigma_{i0}$, consists of an athermal component, $\sigma_{at}$, and a thermal component, $\sigma^*$, i.e.

$$\sigma_{i0} = \sigma_{at} + \sigma^* \tag{5a}$$

The athermal component, $\sigma_{at}$, may in turn be written

$$\sigma_{at} = \sigma_g + \sigma_p + \sigma_s \tag{5b}$$

Here the three components in turn stand for grain size hardening, precipitation hardening and solution hardening. Previous studies of ferritic steel have shown that the thermal component, $\sigma^*$, may approximately be written

$$\sigma^* = \sigma_0 \cdot \left(\frac{\dot{\varepsilon}}{\nu}\right)^{\frac{T}{T_0}} \tag{5c}$$

Here $\sigma_0$, $\nu$, and $T_0$ are material constants. T is temperature, K, and $\dot{\varepsilon}$ is the applied strain rate. For fcc materials σ0 ~ 0 meaning that the thermal component may be neglected.

## Taylors equation for the plastic σ – ε behavior of metals Step 0

Volterras dislocation theory (17) and Taylor's equation (15) still form the base for the research and development carried out in order to increase the knowledge about the relationships between metals mechanical properties and structure.

Equation (4a) gives us an opportunity to formulate a simple theory for polycrystalline metals true plastic stress- strain behavior. What we need to do is to find a physically based expression that describes the variation of total dislocation density $\rho$ ($\varepsilon$) with strain. Taylor started from eqn. (4a) and assumed that the mean free path of mobile dislocations is strain independent, that no dynamic recovery takes place, that the grown-in dislocation density $\rho_0$ can be neglected and that the plastic deformation is homogeneous, see Table 1. He assumed further that dislocation generation is proportional to the Taylor constant, m, and inversely proportional to the Burger vector, b, and the average distance, s0, the mobile dislocations are moving.

***Table1. Assumptions made by Taylor***

| **Nr** | | **Yes** | **No** |
|---|---|---|---|
| 1 | Taylors ekv(4a) is valid | x | |
| 2 | The mean free path of dislocation motion is strain dependent | | x |
| 3 | Dynamic recovery is supposed to take place | | x |
| 4 | $\rho_0$ is taken into account | | x |
| 5 | The plastic deformation process is inhomogeneous | | x |

By proceeding from these assumptions the rate by which dislocations are generated during plastic deformation may be written

$$\frac{d\rho}{d\varepsilon}=\frac{m}{b\cdot s_0} \tag{6a}$$

After integration we have

$$\rho(\varepsilon)=\frac{m}{b\cdot s_0}\cdot\varepsilon+\rho_0 \tag{6b}$$

Here, $\rho_0$ is the grown-in dislocation density at $\varepsilon = 0$. Now, if we assume that $\rho_0 = 0\ m^{-2}$ we obtain after inserting eq. (6b) into eq. (4a) the following approximate expression for the stress-strain behavior of the material.

$$\sigma(\varepsilon)=\sigma_{i0}+M\cdot\varepsilon^{\frac{1}{2}} \tag{6c}$$

and

$$M=\alpha\cdot G\cdot b\cdot\left[\frac{m}{b\cdot s_0}\right]^{\frac{1}{2}} \tag{6d}$$

A comparison between eq. (6c) and Ludwiks eq. (2) shows that an identity exists between the two equations if $\sigma_0 = \sigma_{i0,}$ L = M and q = 0.5. This means that Ludwiks eq. (2) has a physical basis only in the event that q = 0.5.

It may be of interest to note that only a few materials exhibit such a behavior. Some Fe – Si alloys can, however, be passably described by eq. (6c).

Although eq. (6c) has a physical base it is obvious that the simplifying assumption presented above, namely that Taylor eq. (4a) is valid and that the dislocation mean free path is strain independent, s ($\varepsilon$) = s0, not alone leads to a theory that is generally useful. Points 2-5 of the assumptions in Table 1 must therefore also be considered in detail and the results be included in the theory.

For this purpose, we will briefly show how Bergströms theory gradually evolved from the original model of 1965 – Step 1 and Step 2 - to today´s theory of the plastic deformation process of inhomogeneous metallic polycrystalline metals – Step 3.

In his original theory Bergström (14) assumed that the Taylor eq. (4a) was valid and that the mean free path of dislocation motion was strain independent, see points 1 and 2. He added, however, the process of dynamic recovery (Ω) of immobilized dislocations as well as the grown-in dislocation density, $\rho_0$, according to points 3 and 4.

It should be noticed that the value of Ω can be theoretically estimated as well as its variation with temperature and strain rate, see eq.(7e) below.

## THE BERGSTRÖM ORIGINAL THEORY (1960s) – HOMOGENEOUS PLASTIC DEFORMATION – STEP 1

### *Table 2, Assumptions*

| Nr | | Yes | No |
|---|---|---|---|
| 1 | Taylors ekv(4a) is valid | x | |
| 2 | The mean free path of dislocation motion is strain dependent | | x |
| 3 | Dynamic recovery is supposed to take place | x | |
| 4 | ρ0 is taken into account | x | |
| 5 | The plastic deformation process is inhomogeneous | | x |

A reasonable assumption when it comes to dynamic recovery is that such a process, in accordance with the law of natural decay, is proportional to the total dislocation density, ρ(ε). The rate at which dislocations are re-mobilized or annihilated is therefore proportional to the product - **Ω · ρ** (ε). It also seems reasonable to assume that the recovery process is mainly based on re-mobilization at least for metals with high stacking fault energy and many glide systems, e.g. soft steel.

> *Why should Mother Nature unnecessarily ANNIHILATE dislocations – i.e. expend extra energy – and then be forced to create new mobile dislocations, when it is energetically more beneficial to reuse – remobilize – dislocations?*

If we now, in accordance with Taylor, assume that the rate by which dislocations are generated is proportional to $\frac{m}{b \cdot s_0}$ then the rate by which the dislocation density increases may be written

$$\frac{d\rho(\varepsilon)}{d\varepsilon} = \frac{m}{b \cdot s_0} - \Omega \cdot \rho(\varepsilon) \qquad (7a)$$

Ω represents re-mobilization of immobilized dislocations. Integration of eq.(7a) with the constraint that $\rho(0) = \rho_0$ gives the following result

$$\rho(\varepsilon) = \frac{m}{b \cdot s_0 \cdot \Omega} \cdot (1 - e^{-\Omega \cdot \varepsilon}) + \rho_0 \cdot e^{-\Omega \cdot \varepsilon} \qquad (7b)$$

Insertion of eq. (7b) in Taylors´ eq. (4a) yields the following relationship between true stress and true strain.

$$\sigma(\varepsilon) = \sigma_{i0} + \alpha \cdot G \cdot b \cdot \left[ \frac{m}{b \cdot s_0 \cdot \Omega} (1 - e^{-\Omega \cdot \varepsilon}) + \rho_0 \cdot e^{-\Omega \cdot \varepsilon} \right]^{\frac{1}{2}} \qquad (7c)$$

This dislocation theory was developed in the mid – 1960s and was thus based, inter alia, on Taylors eq.(4a) for the relationship between σ(ε) and $\rho(\varepsilon)^{1/2}$.

Taylor´s equation made the work easier because one could focus on models for the strain dependence of the dislocation density instead of directly going to the strain dependence of stress.

By including dynamic recovery (re-mobilization), Ω, in the model as well as the grown-in dislocation density, $\rho_0$, a significantly better agreement between model and experimental data was obtained than when using Ludwiks, Hollomon or Taylor equations – eq.(2), eq.(3) and eq.(4a).

The grown-in dislocation density, $\rho_0$, and the mean free path of dislocation motion, $s_0$, can further on be estimated by experimentally using TEM and $\Omega(\dot{\varepsilon},T)$ may be estimated from the following relationship (14)

$$\Omega = \Omega_0 + \Omega(\dot{\varepsilon},T) \qquad (7d)$$

Where $\Omega_0$ is a constant and $\Omega(\dot{\varepsilon},T)$ varies with T and $\dot{\varepsilon}$ according to the following relationship (14)

$$\Omega(\dot{\varepsilon},T) = (1.85\cdot 10^3 \sqrt{2\cdot D_0})^{\frac{2}{3}} \cdot \exp - \frac{Q_m}{3\cdot R\cdot T} \cdot (\dot{\varepsilon})^{-\frac{1}{3}} \qquad (7e)$$

Where $D_0$, $Q_m$ and R are tabulated data for the self- diffusion of vacancies in the actual metal and $\dot{\varepsilon}$ is the strain-rate.

> We will from now and on assume that Ω is primarily a measure of the remobilization of immobile dislocations.

Although eq. (7c) has been found to give a fairly good description of the plastic deformation process in ferritic steel, the assumption of a strain independent mean free path of dislocation motion is contrary to experimental TEM – observations. This latter type of studies show that s decreases with strain which of course seems reasonable when we consider that the dislocation density in fact increases (14).

Another weakness is of course the assumption that the deformation is homogeneous. This is especially true for cases of advanced high strength steels, e.g. DP steels and martensitic steels. To-day there is a large amount of studies (13, 16) that clearly show that the plastic deformation process, in the latter type of metals, is greatly macroscopically inhomogeneous.

> Let us, however, before we go any further, first show how the Bergström theory change when we face a strain dependent mean free path, s(ε), and at the same time assume that the deformation process is homogeneous – Step 2.

## BERGSTRÖMS FURTHER DEVELOPED THEORY – HOMOGENEOUS DEFORMATION – STEP 2

*Table3. Assumptions*

| Nr |  | Yes | No |
|---|---|---|---|
| 1 | Taylors ekv(4a) is valid | x |  |
| 2 | The mean free path of dislocation motion is strain dependent | x |  |
| 3 | Dynamic recovery is supposed to take place | x |  |
| 4 | ρ0 is taken into account | x |  |
| 5 | The plastic deformation process is inhomogeneous |  | x |

In a second step of further development of his theory Bergström et al introduced a strain dependent mean free path of mobile dislocations, s(ε), and it was assumed (14) that this process was controlled by the law of natural decrease such that s(ε) decreases with strain from an initial value s1 at ε=0 to a value s0 at larger strains, see Table 2. Such a behavior may mathematically be written

$$\frac{ds}{d\varepsilon} = -k(s(\varepsilon) - s_0) \tag{8a}$$

Here k is a material dependent rate constant and after integration we obtain

$$s(\varepsilon) = s_0 + (s_1 - s_0) \cdot e^{-k \cdot \varepsilon} \tag{8b}$$

Eq. (8b) says, therefore, that s(ε) goes from an initial value $s_1$ to a final value $s_0$. TEM studies of the dislocation cell diameters, $d_{\text{cell}}$, show that $s_0 \sim d_{\text{cell}}$, at least in the case of soft single phase ferrite but also in other metals.

By replacing $s_0$ in eq. (7a) with the expression for s (ε) in eq. (8b) we get the following expression for the total dislocation density growth.

$$\frac{d\rho}{d\varepsilon} = \frac{m}{b \cdot s(\varepsilon)} - \Omega \cdot \rho \tag{9a}$$

If we then replace s (ε) in eq. (9a) with the expression for s (ε) in Eq. (8b) we obtain the following expression

$$\frac{d\rho}{d\varepsilon} = \frac{m}{b \cdot (s_0 + (s_1 - s_0) \cdot e^{-k \cdot \varepsilon}} - \Omega \cdot \rho \tag{9b}$$

Unfortunately, eq. (9b) has no analytical solution – and it was because of this fact that Bergström (14) in Step 1 assumed that s was strain independent and equal to $s_0$.This was in the mid-1960s not a bad assumption. The experimental evidence on the strain dependence of the dislocation structure was not well developed and the computers that prevailed at the University of Uppsala were not available for computer-based numerical calculation – at least not for younger graduate students.

To-day, however, eq. (9b) may be easily integrated numerically and by linking this integration process to Taylor´s equation (4a), true stress-strain data can be calculated and adjusted to experimental data.

With the introduction of a strain dependent mean free path of dislocation motion, the models ability to describe the experimental uniaxial tensile test data of single-phase metallic materials has improved significantly. The model is still limited, however, by the fact that no consideration had been given to a possibility of inhomogeneous plastic deformation.

It was also adopted at times, during the initial development stages, that the grown-in dislocation density, $\rho_0$, could be neglected. This is a reasonable assumption only if $\rho_0$ is small, which only applies to single-phase, well annealed metals. For aluminum, copper and soft steel values of the order of ~ $10^{12}$ $m^{-2}$ are recorded.

In the case of modern advanced high strength steels the $\rho_0$ – values are much higher and of the order of ~ $1x10^{14}$ – $1x10^{16}$ $m^{-2}$ because of the martensite transformation. In such cases $\rho_0$ cannot be neglected. The most correct thing to do is therefore to always estimate and include these values in an analysis.

There is, however, always a possibility to try to estimate the dislocation density by the application of TEM.

## A FURTHER DEVELOPMENT OF BERGSTRÖMS THEORY (2000s) – INHOMOGENEOUS PLASTIC DEFORMATION – STEP 3

We shall now proceed to Step 3 and in the theory include the effects of inhomogeneous plastic deformation, see Table 4 (13)

*Table 4. Assumptions – Step 3*

| Nr | | Yes | No |
|---|---|---|---|
| 1 | Taylors ekv(4a) is valid | x | |
| 2 | The mean free path of dislocation motion is strain dependent | x | |
| 3 | Dynamic recovery is supposed to take place | x | |
| 4 | ρ0 is taken into account | x | |
| 5 | The plastic deformation process is inhomogeneous | x | |

However, let us first present a number of experimental observations made in connection with studies of DP steels, martensitic steels and aluminum containing hard particles. We will also show that even single-phase metals as ferrite, aluminum and austenitic steels exhibit some macroscopic inhomogeneity. This latter effect is, however, much weaker than when soft phases are mixed with larger fractions of hard phases.

## EXPERIMENTAL OBSERVATIONS

### DP 800 AND A SINGLE-PHASED FERRITIC STEELE -A4

We have in Step 1 and Step 2 assumed that the plastic deformation process of polycrystalline metals is homogeneous. By studying in detail the DP steels and also other high strength metals it has become clear that the inhomogeneity phenomenon is considerably more substantial and complex than previously realized. Fig. 6a shows the ferrite – and martensite phases in a DP 800-steel containing around 25% martensite. A comparison between the true uniaxial stress-strain curves from the DP 800 steel and from ferritic steel, A4, is presented in Fig. 6b. We see both a higher strength of the DP 800 – steel as well as a much higher initial rate of strain hardening than in the single-phased steel A4.

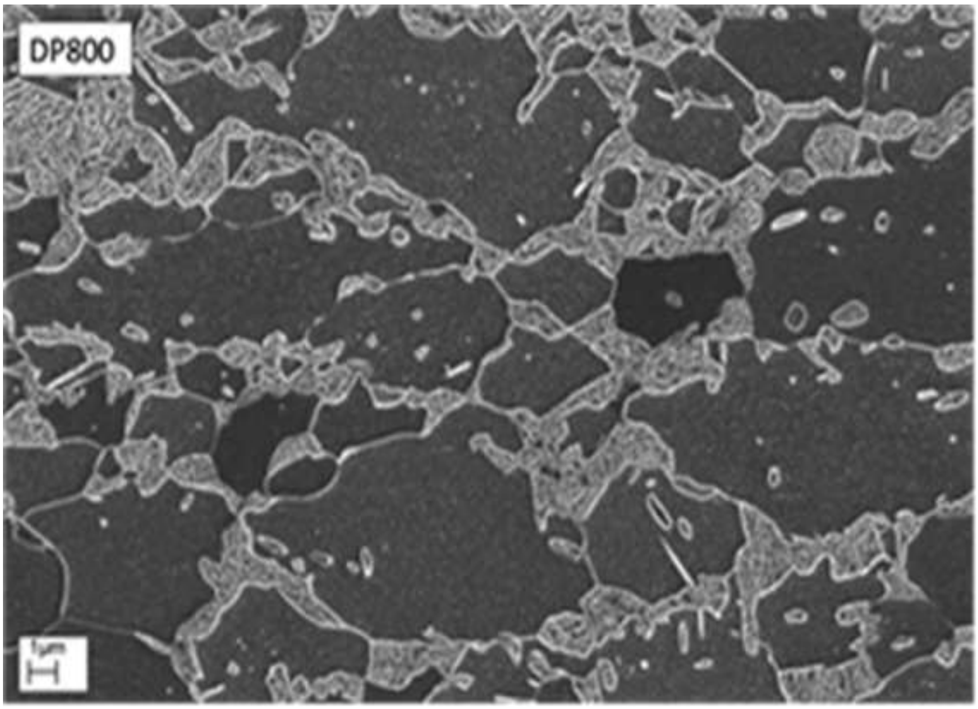

*Fig.6a DP 800 ~25% martensite ~75% ferrite*

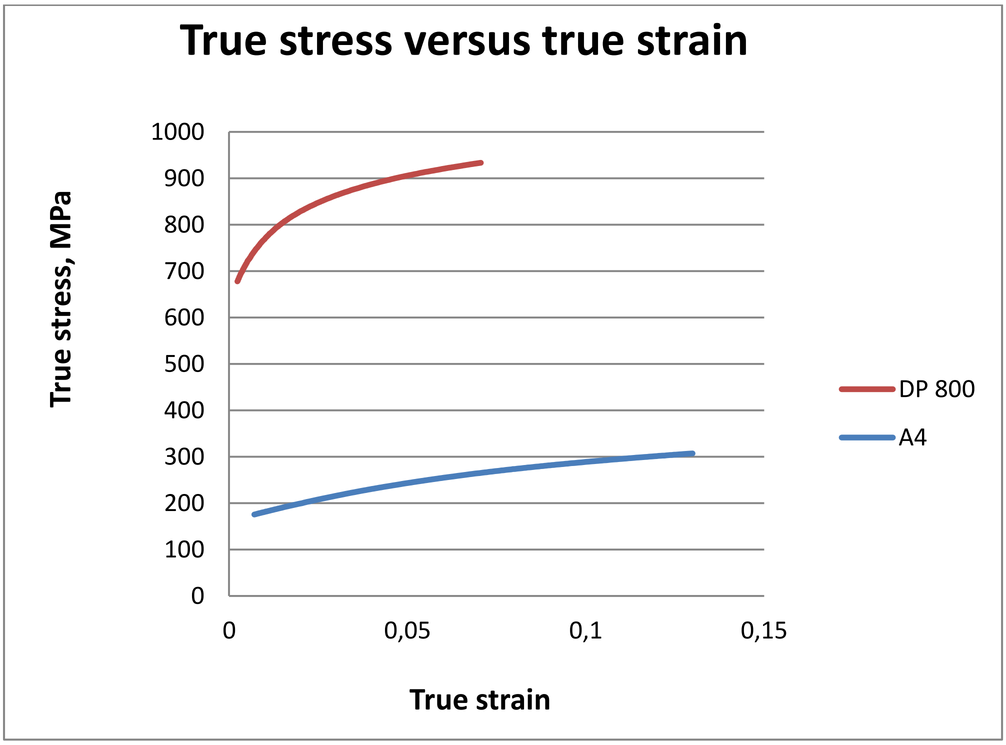

*Fig.6b. True stress-strain curves for DP800 and ferritic steel A*

Detailed structural analyzes of tensile tested DP steel have shown that the plastic deformation is virtually completely localized to the soft ferrite phase, at least for strains up to necking (16) while the martensitic phase shows few signs of plastic deformation in said strain interval. It is also quite clear that the plastic deformation process in the ferrite is strongly inhomogeneous (16). An example of this behavior is seen in Fig. 6c-d showing a EBSD analysis of a DP 800 steel in the undeformed state, Fig. 6c and after having being strained 8% in uniaxial tension, Fig. 6d (13).

The two grains in Fig. 6c of the undeformed material show that the ferrite has undergone some plastic deformation in thin layers, closely located to the surfaces of the martensite particles. This can be related to the martensitic transformation which creates stresses in the ferrite, giving rise to a plastic deformation of the degree 0 – 5 (blue to light green) on the color scale 0 – 10 in close proximity to the martensite. A short distance into the ferrite grains the plastic deformation is significantly smaller, 0 – 2 on the color scale. The plastic deformation is thus initially localized to a relatively thin ferrite layer close to the martensitic particle surfaces.

After an applied plastic deformation of 8%, see Fig. 6d, we see that the plasticizing process has moved inwards the ferritic grains and become larger, 2 – 10 (green to red) on the color scale. The plastic deformation is, however, still inhomogeneous in such a way that it is substantially lower in the grain center than in areas close to the martensite particle surfaces, 1 – 3 (blue to green). The active volume fraction of ferrite, f(ε), participating in the plastic deformation thus increases with applied strain and expands from a small initial value, $f_1$, to a maximum value, $f_0$, which is determined by the volume fractions of ferrite and martensite. It also means that the active volume fraction, f(ε), of a uniaxial test specimen becomes strain dependent which must be taken into account since an increasing active volume fraction, f(ε), leads to a decreasing strain rate in the active volume fraction and hence a decreasing thermal friction stress in this location.

This decrease in strain rate will be accounted for in the theory presented below.

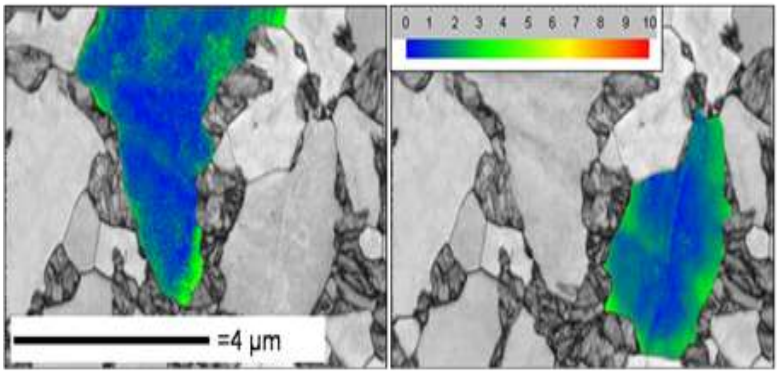

*Fig.6c. EBSD analysis of undeformed DP 800, see text*

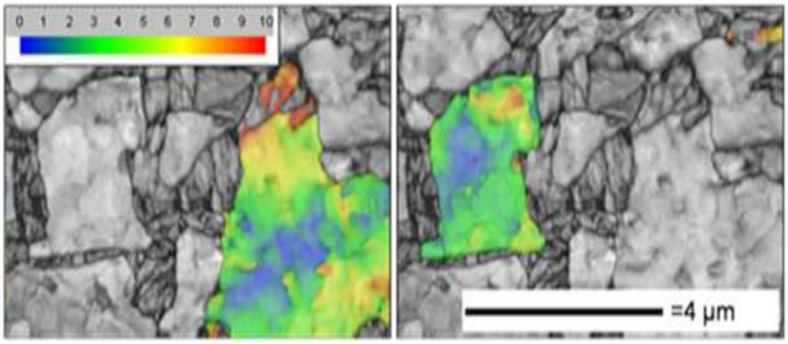

*Fig.6d. EBSD analysis of deformed DP 800 deformed to 8% plastic strain*

Similar observations have been made by Korzekwa et al (14) using TEM studies. They studied a C-Mn-Si DP steels after uniaxial tension 1 – 14%, and showed, inter alia, that the dislocation cells were first formed close to the martensite boarders and that the dislocation cell diameter increases inwards the ferritic grain centers. This supports the conclusion made above that the plastic deformation slowly moves towards the grain centers with increasing strain, see Table 5. It also reveals that a certain volume fraction located in the center of the ferritic grains do not take part in the plastic deformation at all or only to a smaller extent – 0 – 2 on the collar scale.

***Table 5: Table 1: Summary of dislocation substructure development in a C-Mn-Si dual phase steel in tension (14)***

| **True plastic strain (%)** | **Typical ferrite dislocation substructures** | **Variation of the substructure within a typical ferrite grain** |
|---|---|---|
| 0 | Very low average dislocation density | High dislocation density adjacent to martensite |
| 1 | No cells; a few straight, planar dislocation walls | Dislocation density higher near martensite |
| 2 | Incipient cells; many long, straight walls | Cell structure generally forms first near martensite |
| 7 | Well-developed cell structure; thick cell walls | Cell size smaller near martensite (~0.4μm) than away from martensite (~0.7μm) |
| 14 | Well-developed cell structure with many straight, thin cell walls | Cell sizes approximately the same as for 7 pct strain |

Fig. 7a shows experimental uniaxial true stress-strain curves for three DP – steel, namely DP500, DP 800 and DP 1000. It is easily noted that, for this type of steel, the hardness as well as the rate of strain hardening increases with increasing martensite content. It should also be noted that the initial rate of strain hardening is more forceful than that at higher strains.

This increase in strain hardening is intimately related to the localization of the plastic deformation process which is caused by the inhomogeneous state – i.e. localization to the soft ferrite. In DP steels, therefore, the rate of strain hardening is controlled partly by the martensite content and partly by the inhomogeneous localization in the ferrite. DP1000 has the highest martensite content and consequently the lowest ferrite content. Together with the localization in the ferrite DP1000 therefore exhibits a higher rate of strain hardening than the DP 800- and DP500 steels. This is thus a possible, and reasonable, basic explanation to why an excellent ductility may be maintained at such a high strength.

In the theoretical analysis, presented below, we will in deeper detail show how various physical parameters are influenced by this type of inhomogeneity.

## MARTENSITIC STEEL M1700

Also the three martensitic steels in Fig. 7a, namely M1200, M1500 and M1700 show different strengths and different rates of strain hardening and it also holds that the rate of strain hardening increases with increasing strength.

A detailed study of M1700, which is the hardest of the three M-steels, indicates that the total active volume fraction of “the ferrite” is about 5% and localized to areas intimately close to the old austenite grain boundaries, see Fig. 7b. The initial active volume fraction is about a factor of 25 smaller, see the theory section below. It should be noticed that what we call “ferrite” here is softened martensite localized in close contact with the old austenite grain boundaries – see details below.

A reasonable assumption when it comes to the increase in the rate of strain hardening is to assume that both the initial as well as the total local active volume fractions of “ferrite” decrease with increasing martensite content. However, we should not forget that the mean free path, s(ε), of mobile dislocations should also decrease with decreasing active volume fraction, thus further increasing the rate of strain hardening.

The fact that the plastic deformation process is localized to small active volume fractions of the tensile test specimen also leads to an increase in the local strain rate as compared to the applied strain rate. This effect must also, as pointed out above, be considered in a detailed analysis of inhomogeneous plastic deformation.

The localization of the active volume fraction “ferrite” to the old austenitic grain boundaries is shown in Fig. 7b, where the red markings indicate austenitic grain boundary areas who have actively participated in the deformation process. The applied stress is horizontal and it is evident that there is a clear tendency among the red marked grain boundaries to form an angle about $45^0$ with the tension direction and thus exhibiting a greater tendency for the plasticity effect than other grain boundaries. This is of course a result of the fact that the shear stress reaches a maximum under such conditions. There is also a tendency of grains to form blocks where each block contains a plurality of undeformed old austenitic grain boundaries.

Each block, however, seems to be surrounded by grain boundary areas which exhibit a sharp “blurr-effect” (local plastic deformation). The block diameter varies, however, with a mean value of about 10 μm. One possible interpretation is that the block boundaries represent some type of “low energy areas”, and that the plastic deformation process is localized there. With the aid of a “line-scan function” it was verified that the martensite exhibited few signs of plastic deformation for strains up to necking. In Fig. 7c the uniaxial $\sigma - \varepsilon$ stress strain curves for the martensitic steel M1700 together with that from the single-phase ferritic steel A4 are shown. The difference in strength, as well as rate of strain hardening is significant.

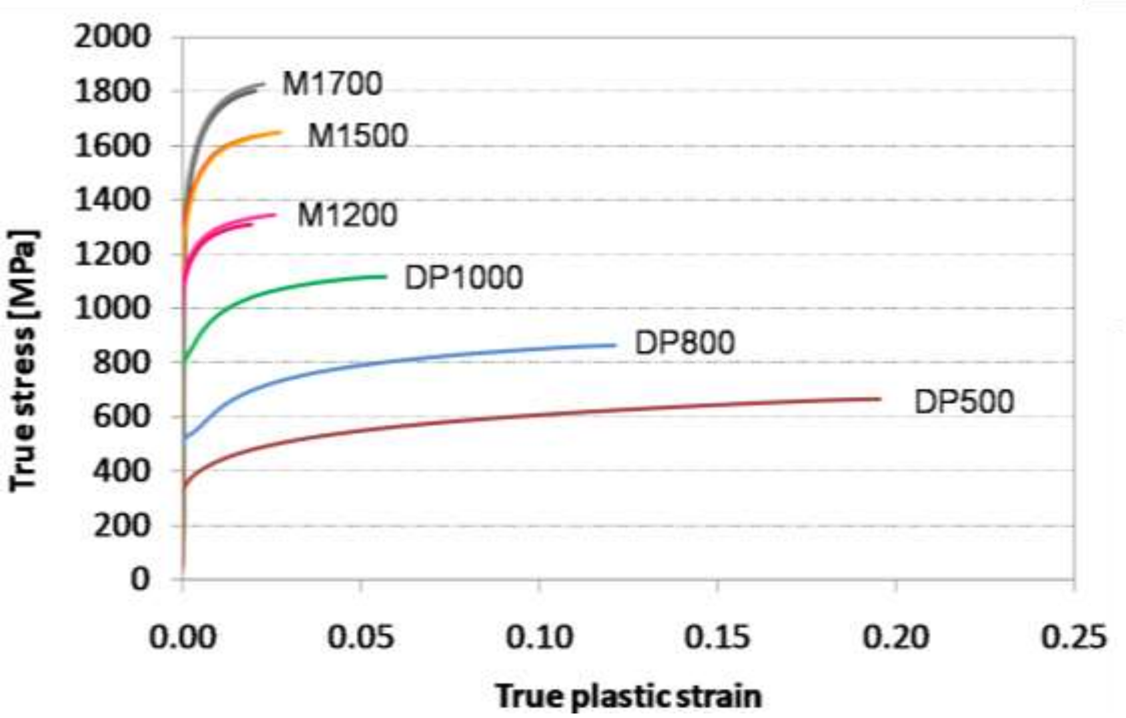

*Fig.7a. True uniaxial stress-strain curves for three DP-steels and three martensitic steels with different strength strained to necking. Note that the strength and the rate of strain hardening increases with increasing strength.*

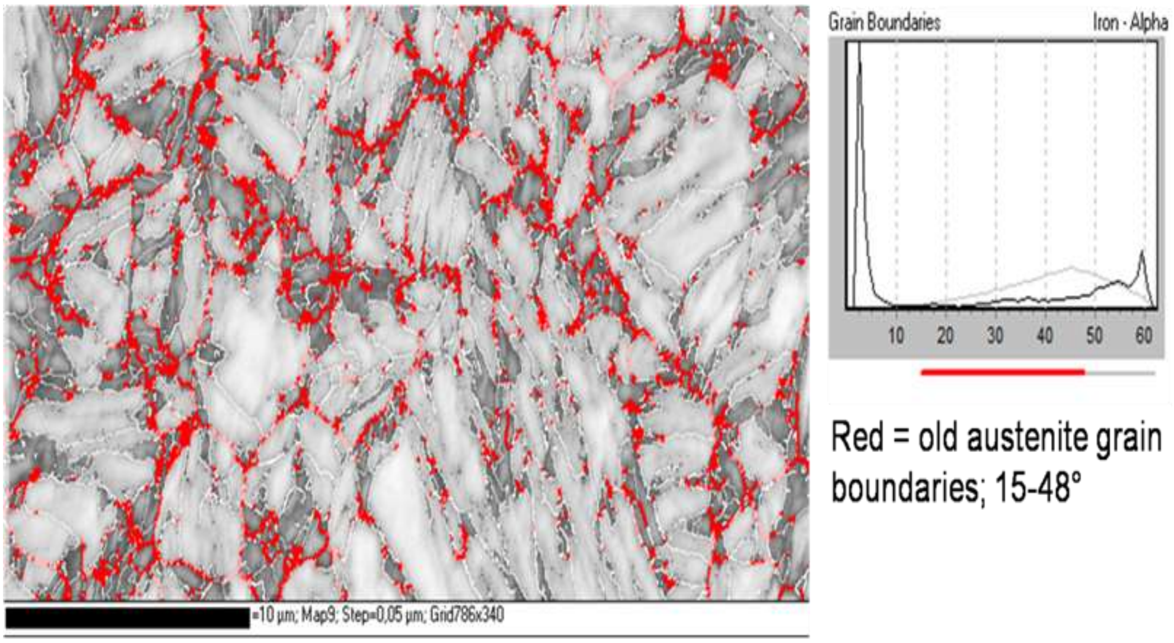

*Fig.7b.EBSD - analysis of grain boundaries. The old austenitic grain boundaries, marked with red, are identified as sites where the plastic deformation initiates and propagates. This indicates that the localization of the plastic deformation process is strong. We can also see a clear tendency of block formation of grains where the grain boundaries that define the blocks are heavily deformed. The applied stress is horizontal. The block diameter has been estimated to be ~10 µm.*

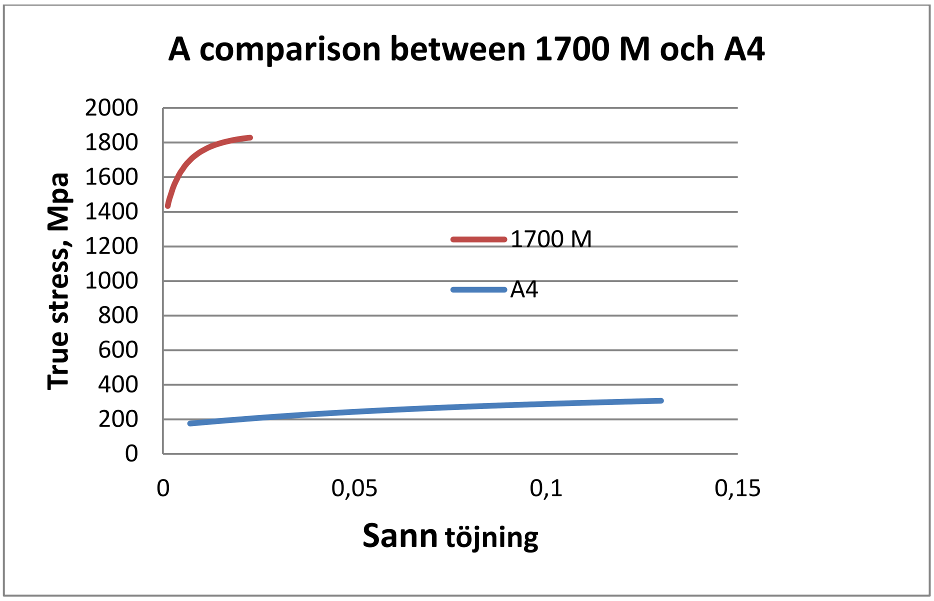

*Fig. 7c A comparison between the uniaxial stress-strain curves for the martensitic steel M1700 and the single-phase ferritic steel A4.*

## ALUMINUM ALLOY - AA3003 AND Al – 0.052%Ti

We have so far focused on DP steels and martensitic steels but also other metals, such as for instance aluminum exhibit an improved strength and strain hardening rate if hard particles of size 1 – 10 μm are added to the substructure. This is clearly illustrated by Fig. 8a where uniaxial stress-strain curves from a single-phase aluminum alloyed with 0.052%Ti and an aluminum alloy containing hard particles, AA3003 are presented.

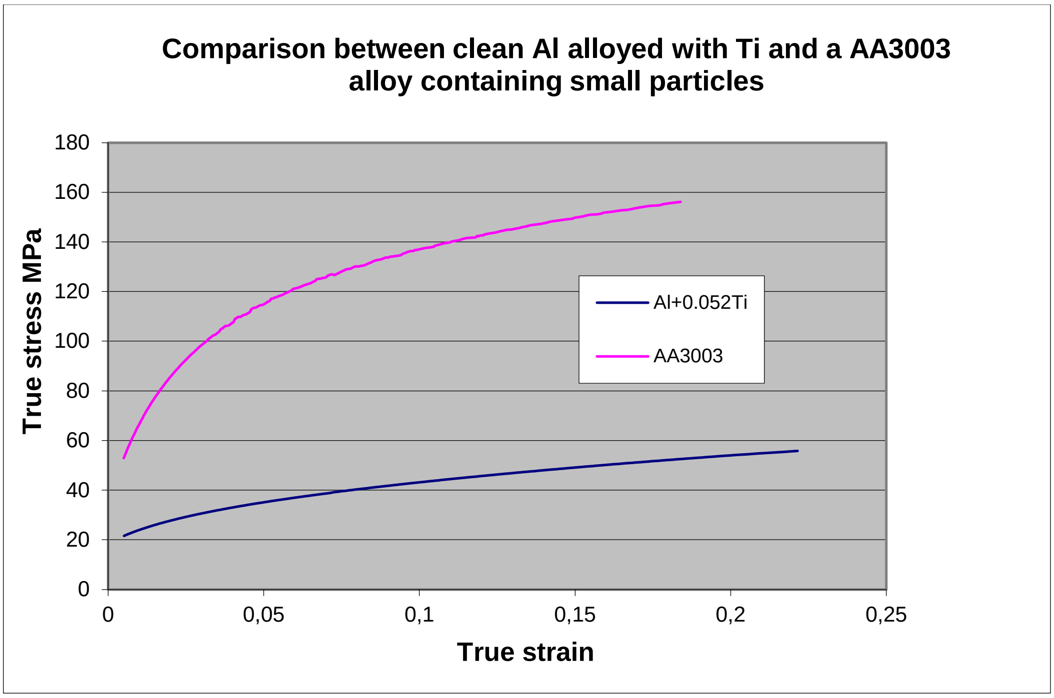

*Fig.8a. True uniaxial stress – strain curves from polycrystalline, single-phase Al alloyed with 0.052%Ti and an Al-alloy, AA3003, containing ~ 8% hard particles of the size 1 – 10 µm*

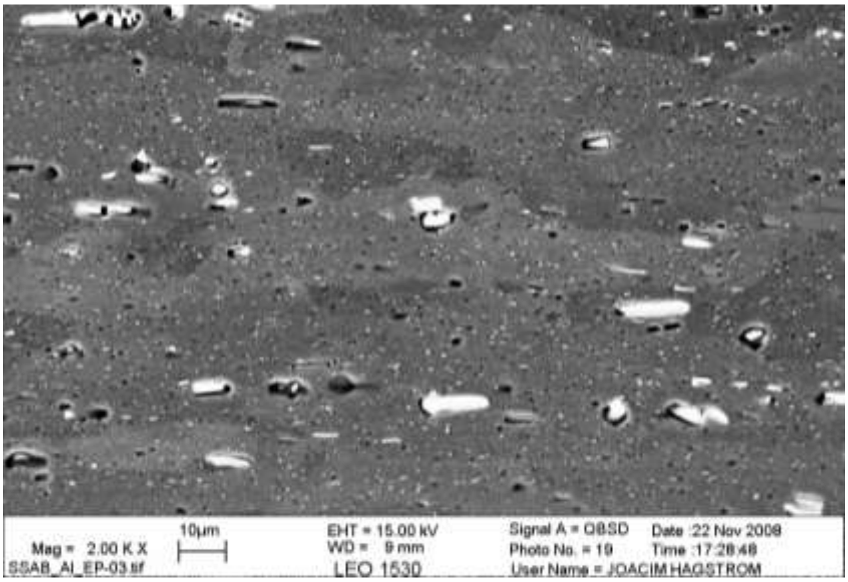

*Fig.8b. Aluminum containing a volume fraction of ~ 8% hard particles of diameter 0.3 – 10 µm*

The volume fraction of hard particles is approximately 8%. We can see in Fig. 8a that AA3003 has a considerably larger rate of strain hardening than the single-phase Al. The result will be a higher strength and a higher ductility. Also this positive behavior is a result of inhomogeneous plastic deformation similar to that in pure ferrite containing a hard second phase, see Fig. 7c and the analysis presented in the theory section below.

## AUSTENITIC STAINLESS STEEL

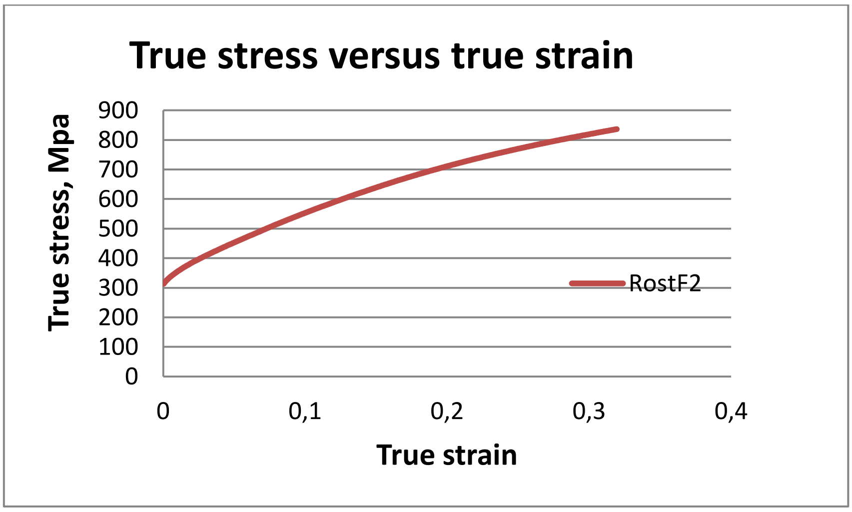

*Fig. 9 True plastic stress-strain curve for commercial austenitic steel*

As has already appeared from the true stress-true strain curves of single-phase ferrite, A4, in Fig. 6b and single-phase aluminum in Fig. 8a, it is quite clear that the initial rate of strain hardening is significantly lower than in the steels DP 800, see Fig. 7a, 1700M, see Fig. 7c and AA3003, see Fig.8a. Also the austenitic steel, Fig. 9, initially shows a lower rate of strain hardening because of the absence of large hard particles. Experimental data therefore strongly support the idea that the increased rate of strain hardening and increased strength in these latter materials containing a mixture of soft and hard phases emanate from a decreasing volume fraction of softening active phase and that this fraction initially is small but growing with increasing strain.

## THE INHOMOGENITY OF METALLIC MATERIALS – GENERAL

We will now further-develop Bergström dislocation model to take into account the experimental fact that the plastic deformation process in high strength steels as well as single-phase metals of type soft steel and aluminum is macroscopically inhomogeneous. The inhomogeneous effect is, however, more pronounced in the high strength materials and is caused by various types of defects.

Metallic commercial metals are far from defect-free and a frequently used way to classify the most common defects is the following:

***Point defects:*** This type of defects affects in various ways the movements of dislocations. The vacancies are created inter alia during heat treatments and plastic deformation and their density increases with increasing plastic deformation**.** This also increases a material´s self-diffusion. Since inhomogeneity causes an increased localization of the plastic deformation process the result will lead to an enhanced local vacancy concentration and hence an increase in local diffusion. This might influence the local properties even at moderate temperatures and give rise to various types of effects that ought to be further investigated.

Substitutional atoms, as well as interstitials like C and N in ferrite, give rise to solution hardening.

***Linear defects:*** Dislocations are created by multiplication which gives rise to plastic deformation and strain hardening. A localization of the plastic deformation process as in inhomogeneous materials therefore leads to a localized strain hardening.

***Strain ageing:*** The interstitials carbon and nitrogen in steel will contribute to solution hardening but also to strain ageing, both static and dynamic. In the case of dynamic strain ageing, mobile dislocations are captured by the solute C or N- atoms and give rise to an inhomogeneous deformation – the so called serrations. In static strain ageing in steel these interstitials lock the immobilized dislocations and the possibility of remobilization of these dislocations is reduced or eliminated. This indirectly leads to an increased deformation hardening after ageing. If these processes take place during inhomogeneous conditions the effect is enhanced.

***Parting faces:*** Grain boundaries, subgrainboundaries and phase boundaries affect the movement of dislocations and the plastic behavior of metals. Grain boundaries give rise to the so-called Petch-Hall effect. Subgrainboundaries have a similar strength enhancing effect. The presence of different phases with varying hardness, separated by their surfaces, gives rise to a significant macroscopic inhomogeneous plastic deformation.

***Residual stresses:*** These stresses have macro-, micro- and sub-micro propagation and occur in all metallic materials that have been mechanically processed and/or heat treated. This type of stresses can easily be triggered when a tensile stress is applied and can thus help to generate initial, local outbreaks of plastic deformation.

***Texture:*** A textured materials easily contributes to inhomogeneous plastic deformation. The more palpable the texture is all the more apparent becomes the inhomogeneity. Variations in grain size also easily generate inhomogeneity.

***Volume effects I:*** Small and medium sized particles contribute to particle hardening. They may even give rise to inhomogeneous plastic deformation at macro-, micro- and sub-micro level dependent on particle size and distribution.

***Volume effects II:*** Large volume fractions of different hard phases – e.g. martensite, bainit or perlite – in a soft ferrite phase leads to a macroscopically inhomogeneous plastic deformation localized inside the ferrite phase – at least for uniaxial strains below that to necking. Hard larger particles in soft fcc phases like copper and aluminum contribute in a similar manner to an increased inhomogeneous plastic deformation.

***General:*** The large amount of new experimental techniques developed in recent decades has made it possible to identify new important details about the plastic deformation process. One such observation is that the latter process is considerably more macroscopically inhomogeneous than previously thought. This is especially true for the new advanced high-strength steels and other materials formed by mixtures of soft and hard phases.

## UNIAXIAL STRAINING

A major problem associated with the evaluation of uniaxial tensile test data is that it is assumed according to standard procedures that the entire volume of the test specimen participates in the plastic deformation process – see Appendix 1.

Such an assumption is namely fundamentally flawed for inhomogeneous materials. Telling examples are the modern DP steels; see above, where the plastic deformation is localized to the soft ferrite for strains up to necking. The martensite remains largely unaffected by plastic straining. It also holds that the plastic deformation process in the ferrite is inhomogeneous.

(Although we have already pointed to this fact above, we want to remind the reader about some critical points before we start to introduce the new theory which makes it possible to calculate the local strains, εl, from the global strains, εg, recorded in the tensile test):

> Example: DP steel. The plastic deformation starts in the ferrite and is initially located intimately close to the martensite phase boundaries. It then propagates slowly inwards the soft ferrite grains with increasing applied strain. We thus have an, with increasing strain, increasing active volume fraction, f(ε), of the sample that takes part in the process. The initial local rate of strain hardening in the test rod is thus much larger than at later stages of deformation. This explains the experimentally observed high rate of initial strain hardening in this type of materials.
>
> To adapt an unadjusted σ – ε model or an empirical relationship to inhomogeneous experimental tensile test data usually leads to errors in the conclusions drawn from the obtained results. This type of inhomogeneity problems has mostly been neglected in the literature at least in the case of macroscopic inhomogeneity. In order to be able to make a more correct analysis it is necessary to correlate the local strains with the corresponding global strains in a tensile test.
>
> In the case of pure single-phase metals, the inhomogeneity effect is comparatively small and may be neglected.

Let us now, in some detail, consider the plastic deformation of inhomogeneous metallic polycrystalline metals. We will start by deriving a theory and then step by step show that it can adequately describe the uniaxial true stress-true strain behavior of various inhomogeneous as well as homogeneous metals.

For the derivation of this model we will proceed from Bergströms theory for homogeneous plastic deformation – step 2, see Fig. 10a.

The resulting theory will be tested on a DP 800 steel , a 1700M martensitic steel and an aluminum alloy, AA3003, containing hard large particles of size 1 – 10 μm. We will also demonstrate that single-phase soft metals like soft ferritic steel, aluminum and austenitic stainless steel are also they to some extent inhomogeneous and may be described by the new theory. In the latter case the inhomogeneity is comparatively small and may be neglected.

We will now introduce the new, further-developed dislocation theory for various types of inhomogeneous metals and alloys.

# A DISLOCATION THEORY FOR THE PLASTIC DEFORMATION BEHAVIOR OF INHOMOGENEOUS METALS IN UNIAXIAL STRAINING

## General introduction:

We will now show how the Bergström homogeneous dislocation theory –Step 2- can be further developed to include inhomogeneous plastic deformation – Step 3 – see Table 4. To do this we will proceed from Fig.10 a, where a schematic picture of the different processes involved in the homogeneous state are shown.

## Basic assumptions:

- The theory includes a correction for inhomogeneous plastic deformation and holds for uniaxial straining up to necking

- We proceed from the classical view that dislocations behave as edge dislocations, screw dislocations and as combinations thereof. We further assume that dislocations are created, moving, cross-slipping, multiplying, immobilizing and remobilizing in a traditional way.

- We assume that the deformation starts in the soft phase close to the phase interfaces between the soft and the hard phases, partly as a result of the presence of residual stresses caused by phase transformations and processing routines, and partly because of compatibility conditions giving rise to stress concentrations in the affected areas. The strain hardening process is thus initially localized to the soft phase near the hard phase surfaces. As a result of the high strain hardening rates in these areas the plastic deformation process is forced to move inwards the soft grains with increasing applied stress due to a lower hardness resistance there.

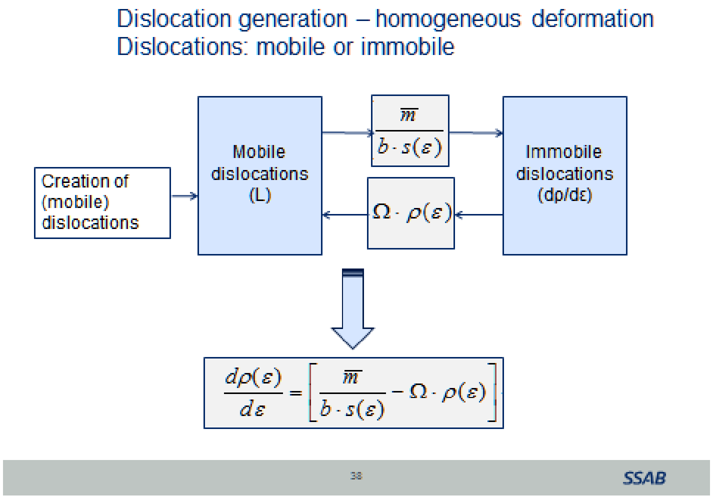

*Fig.10a. Schematic presentation of Bergströms dislocation theory–homogeneous deformation – Step 2*

- The inhomogeneous material is assumed to consist of the following volume fractions:

1. A hard phase, $f_h$, which is deformed elastically, but not plastically
2. An active soft phase, f(ε), which deforms elastically and plastically
3. A non-active soft phase, $f_{udef}$, which deforms elastically, but gradually, with increasing strain, becomes plastically active (compare with Lüder´s strain).

- The plastically undeformed fraction soft phase, $f_{udef}$ (ε)=$f_0$-f(ε), i.e. the one that continually decreases with increasing strain, may be regarded as temporarily hard since it does not, in that stage, take active part in the plastic deformation process and may in that respect be compared with the hard phase fraction. For this reason, stress concentrations may also form between deformed and non-deformed soft phases. This is reminiscent of the Lϋder´s phenomenon of ferrite in which a movable front separates the deformed soft phase from a non-deformed one.

- The plastic deformation process may not necessarily start simultaneously in all soft volume fractions but can randomly and continuously be initiated at various locations during the deformation process – also this type of behavior is comparable with the Lϋder´s phenomenon where several Lϋder´s bands can be formed, move and stop with time.

- Although the dislocation density can exhibit local variations, as a result of the inhomogeneous plastic deformation, we assume that Taylor´s eqn. (1) applies to the dislocations average in the active soft volume fraction.

- The mean free path of dislocation motion is assumed to decrease exponentially with strain in accordance with eq. (8b).

## The active volume fraction, f(ε)

We assume that the load applied on an inhomogeneous material is distributed throughout the whole sample volume, i.e. on the hard volume fraction, $f_h$,, on the active soft phase, f(ε), and on the non-deformed soft phase, $f_{udef}$.

Now, if the stress acting on the active soft phase is, $\sigma_f$ , then the same stress is acting on the other two fractions but only in an elastic manner. The global stress, σ, may therefore be written

$$\sigma = (f_h + f(\varepsilon) + f_{udef}) \cdot \sigma_f \tag{10}$$

Where $f_h + f(\varepsilon) + f_{odef} = 1$.This means that the global stress, σ, is equal to the local stress, $\sigma_f$, which is acting on the active volume fraction soft material.

The plastic strain dependence of the dislocation density, ρ, in the active phase may according to the chain rule be written

$$\frac{d\rho}{d\varepsilon_f} = \frac{d\rho}{d\varepsilon} \cdot \frac{d\varepsilon}{d\varepsilon_f} \tag{11}$$

Where, $\varepsilon_f$, is the local strain in the soft phase and ε is the global strain. The global strain, ε, is because of the macroscopic inhomogeneity related to the local strain, $\varepsilon_f$, as

$$d\varepsilon \cong f(\varepsilon) \cdot d\varepsilon_f \tag{12}$$

The global strain dependence of the total dislocation density for a macroscopically inhomogeneous material may thus be written

$$\frac{d\rho(\varepsilon)}{d\varepsilon} = \frac{1}{f(\varepsilon)} \cdot \left[ \frac{m}{b \cdot s(\varepsilon)} - \Omega \cdot \rho(\varepsilon) \right] \tag{13}$$

We will further on assume that the strain dependence of, f(ε), is based on “natural growth” and that it may be written

$$\frac{df(\varepsilon)}{d\varepsilon} = r \cdot (f_0 - f(\varepsilon)) \tag{14}$$

Where r is a material parameter controlling the rate at which the process goes on. After integration the following relationship is obtained

$$f(\varepsilon) = f_0 + (f_1 - f_0)\cdot e^{-r\cdot\varepsilon} \qquad (15)$$

Here $f_1$ is the initial fraction soft phase participating in the deformation process and $f_0$ is the total volume fraction soft phase. Hence, f(ε), starts from $f_1$ and grows with increasing strain towards $f_0$.

Proceeding from eq. (12), the relationship between the local strain, $\varepsilon_f \sim \varepsilon_l$, and the global strain, $\varepsilon \sim \varepsilon_g$, may therefore approximately be written

$$\varepsilon_l \cong \frac{\varepsilon_g}{f_0 + (f_1 - f_0)\cdot e^{-r\cdot\varepsilon_g}} \qquad (16)$$

In a homogeneous material it holds that $f_1=f_0=1$with the result that $\varepsilon_l = \varepsilon_g$. In an inhomogeneous material, on the contrary, it holds that $f_1 < f_0 < 1$ with the result that $\varepsilon_l > \varepsilon_g$. In the latter type of material it also holds that $\varepsilon_l \sim \varepsilon_g/f_1$ at small $\varepsilon_g$ – values and $\varepsilon_l \sim \varepsilon_g/f_0$ at large $\varepsilon_g$ – values. We will return to these facts in a later section.

A further development of Bergströms homogenous dislocation model to the inhomogeneous case leads to the result depicted in Fig. 10b.

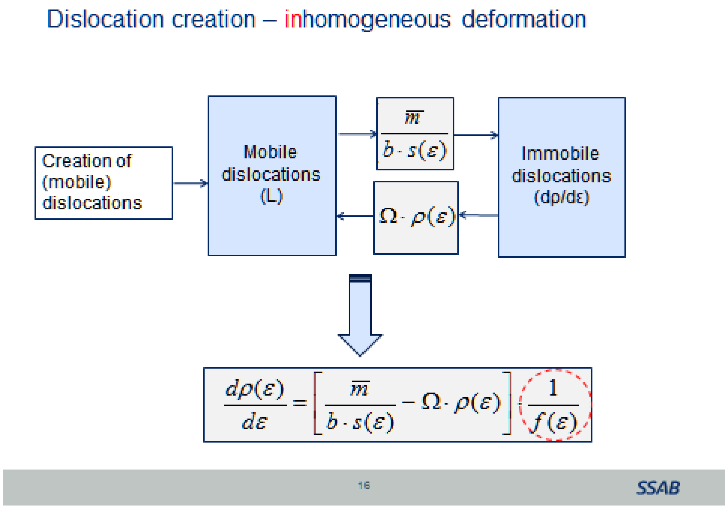

*Fig. 10b. Schematic presentation of Bergströms dislocation-theory – inhomogeneous deformation – step3*

Now, if we replace s(ε) and f(ε) in Fig.10b with the expressions in eq.(8b) and eq.(15) we obtain the following expression for the rate by which dislocations are generated in uniaxial straining

$$\frac{d\rho}{d\varepsilon} = \frac{1}{f_0 + (f_1 - f_0)\cdot e^{-r\cdot\varepsilon}}\cdot\left[\frac{m}{b\cdot(s_0 + (s_1 - s_0)\cdot e^{-k\cdot\varepsilon}} - \Omega\cdot\rho\right] \qquad (17)$$

Eq. (17) gives us the global strain dependence of an inhomogeneous material expressed in the parameters of the soft phase, i.e. a description of the continuous localization process in an inhomogeneous material consisting of a volume fraction of soft phase that undergoes plastic deformation and a volume fraction of hard phase that does not deform plastically.

A comparison between eq.(17) and Bergströms original theory for homogeneous plastic deformation of single-phase materials, eq.(9b) shows that eq.(17) transforms to eq.(9b) if $f_0 = f_1 = 1$, i.e. if we assume that $f_h = 0$ and that the plastic deformation is homogeneous.

Proceeding from this line of reasoning, we can now in terms of global strain, mathematically and physically estimate how the plastic deformation progresses up to necking in inhomogeneous materials. In practice this means that the deformation is inhomogeneous with local strain gradients in the soft phase. It is within this context that the inhomogeneity factor, f(ε), can be seen as a liberating factor since it makes it possible via eq. (16) to relate the global strain, $\varepsilon_g$, evaluated from the uniaxial tensile test to the local strain, $\varepsilon_l$, which is the actual average strain determining the local work hardening and thus also the global work hardening. The results we obtain are based on averages of the plastic deformation processes going on both inside the individual grains in the soft phase as well as in between the grains in the soft phase. Although the plastic deformation process can vary greatly, both locally and macroscopically, the function f(ε) is at all times governed by the average volume fraction that actively participates in the deformation process.

The parameter values that we obtain in the adaption of the theory to experimental uniaxial stress-strain data are thus averages, based on the local deformation. We can, therefore, based on them, make reasonable physical assessments of how the material parameters affect the plastic deformation process. It thereby becomes easier to understand the physical impact that a materials inhomogeneity has on the macroscopic properties and how to proceed to further develop and optimize the material properties for various applications.

We may also simply estimate the local strains proceeding from the global strains $\varepsilon = \varepsilon_g$ and, $f(\varepsilon_g)$, see eq.(16).

## Fitting the inhomogeneous theory to experimental data– Phase 3

### Demonstration example - DP800

A special Matlab-subroutine, which is based on Matlab Curve Fitting Toolbox, has been developed to fit the model – eq.(4a).and eq.(17) – to experimental uniaxial true stress – true strain data. The parameters start values are chosen partly from previous experimental results and partly from previous experience.

Each fit gives rise to a result similar to that presented in Fig (11a) where we have chosen the DP 800 steel as an example. It might also be suitable, at this stage, to make some extra comments regarding the fitting procedure as such as well as to the results obtained in this fitting procedure:

- *Since the plastic deformation process goes on in the ferritic phase it holds that:* $\alpha = 0.5$, $G=80000$ *MPa*, $b=2.5E\text{-}10$ *m*, $m=2$, $\sigma_0=1000$ *MPa*, $T_0=2680K$, $\nu=1E9s^{-1}$, $T=296K$ *and* $\dot{\varepsilon} = 0.0104\ s^{-1}$
- *The following parameter are allowed to vary:* $\Omega$, $\rho_0$, $f_1$, $f_0$, $r$, $s_1$, $s_0$, $k$, $\sigma_{at}$
- *The small figure at the top left in Fig.11a illustrates the fitting of the theoretical σ-ε curve to the experimental data for the DP 800 steel. At the bottom of this small figure the results from the fit regarding the true strain to necking,* $\varepsilon_n = 0.083$ *and corresponding true stress,* $\sigma_n = 946.0$ *MPa are presented. These values are in good agreement with the experimental ones.*
- *The corresponding variation of the total dislocation density,* $\rho(\varepsilon)$*, with strain is shown in the upper middle figure. The grown-in dislocation density is calculated to be* $\rho_0=1.42E14\ m^{-2}$*.*
- *The upper right figure shows the errors in the fit as a function of strain. The statistical average error is estimated to be 0.15 MPa. The initial errors are, however, larger (~ 2MPa) and decrease with strain toward the value (~ 0.2 MPa). This behavior is presumably connected to a successive release of larger residual stresses and other types of stress concentrations.*

- *The lower left part of the figure shows the table exhibiting the parameter values obtained in the fit. The parameter values marked by a black dot have known values and are kept constant through the fit. The other parameter values have been allowed to vary freely until the error in the fit reaches a minimum value.*
- *It is possible in the fitting procedure to lock one or more parameter values. It is also possible to diminish the parameters sensitivity of fit in a scale of 1 – 10 by special marking. This latter function has not been used in the present analysis.*
- *The table to the right shows the corresponding values at the last previous adjustment, 100 cycles earlier. We see here that the differences at this stage between the two table´s values are small and negligible why further runs become unnecessary.*
- *The upper small figure to the right of the 100 cycles table, shows how the active volume fraction of ferrite, f(ε), varies with strain. The values obtained for fm, $f_1$, $f_0$ are 0.273, 0.152 and 0.727 respectively. The r -value is estimated to be 20.66.*
- *The mean free path of the mobile dislocations, s(ε) as a function of strain is presented in the upper, to the right positioned, small figure. We can see that s(ε) is decreasing with strain from $s_1$=7.584E-7 m to $s_0$=5.17E-7 m. The rate parameter k=305.4.*
- *The small figure to the rightmost shows how the total friction stress, $\sigma_{i0}=\sigma_{at}+\sigma^*$ varies with strain. The athermal component $\sigma_{at}$=434 MPa. The thermal component varies with strain from 508-496=12 MPa.*

## *DP 800*

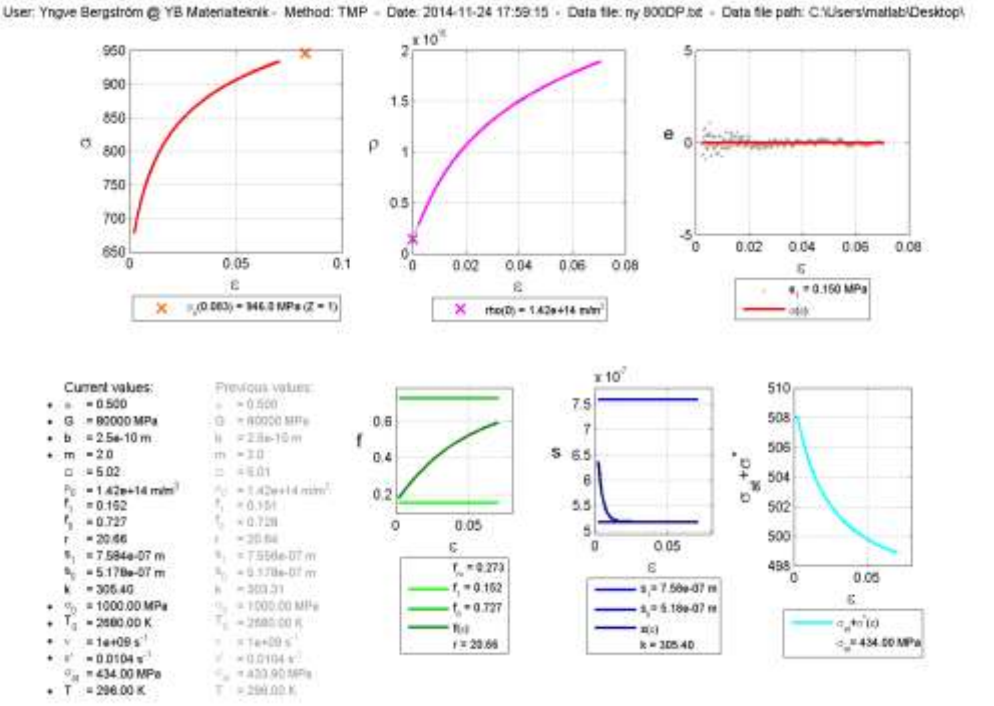

User: Yngve Bergström @ YB Materialteknik - Method: TMP - Date: 2014-11-24 17:59:15 - Data file: ny 800DP.txt - Data file path: C:\Users\matlab\Desktop\

| | Current values: | Previous values: |
|---|---|---|
| • | $\alpha$ = 0.500 | $\alpha$ = 0.500 |
| • | G = 80000 MPa | G = 80000 MPa |
| • | b = 2.5e-10 m | b = 2.5e-10 m |
| • | m = 2.0 | m = 2.0 |
| | $\Omega$ = 5.02 | $\Omega$ = 5.01 |
| | $\rho_0$ = 1.42e+14 m/m³ | $\rho_0$ = 1.42e+14 m/m³ |
| | $f_1$ = 0.152 | $f_1$ = 0.151 |
| | $f_0$ = 0.727 | $f_0$ = 0.728 |
| | r = 20.66 | r = 20.64 |
| | $s_1$ = 7.584e-07 m | $s_1$ = 7.556e-07 m |
| | $s_0$ = 5.178e-07 m | $s_0$ = 5.178e-07 m |
| | k = 305.40 | k = 303.31 |
| • | $\sigma_0$ = 1000.00 MPa | $\sigma_0$ = 1000.00 MPa |
| • | $T_0$ = 2680.00 K | $T_0$ = 2680.00 K |
| • | $\nu$ = 1e+09 s⁻¹ | $\nu$ = 1e+09 s⁻¹ |
| • | $\varepsilon'$ = 0.0104 s⁻¹ | $\varepsilon'$ = 0.0104 s⁻¹ |
| | $\sigma_{at}$ = 434.00 MPa | $\sigma_{at}$ = 433.90 MPa |
| • | T = 296.00 K | T = 296.00 K |

***Fig.11a. Fitting of the inhomogeneous theory to DP800 steel – for a compilation of all parameter values, Table 6***

Below are the individual results obtained from the adaptation of the inhomogeneous theory to the experimental uniaxial tensile test curves presented for DP800-steel, Fig 11a, the martensitic1700M-steel, fig. 11b, a ferritic mild steel A4, fig. 11c, a particle-reinforced Al - AA3003, Fig. 12a, a high purity Al+0,052% Ti, Fig. 12b, and an commercial austenitic stainless steel, Fig 13.

For the compilation of parameter values, see Table 6.

## MARTENSITIC 1700 M

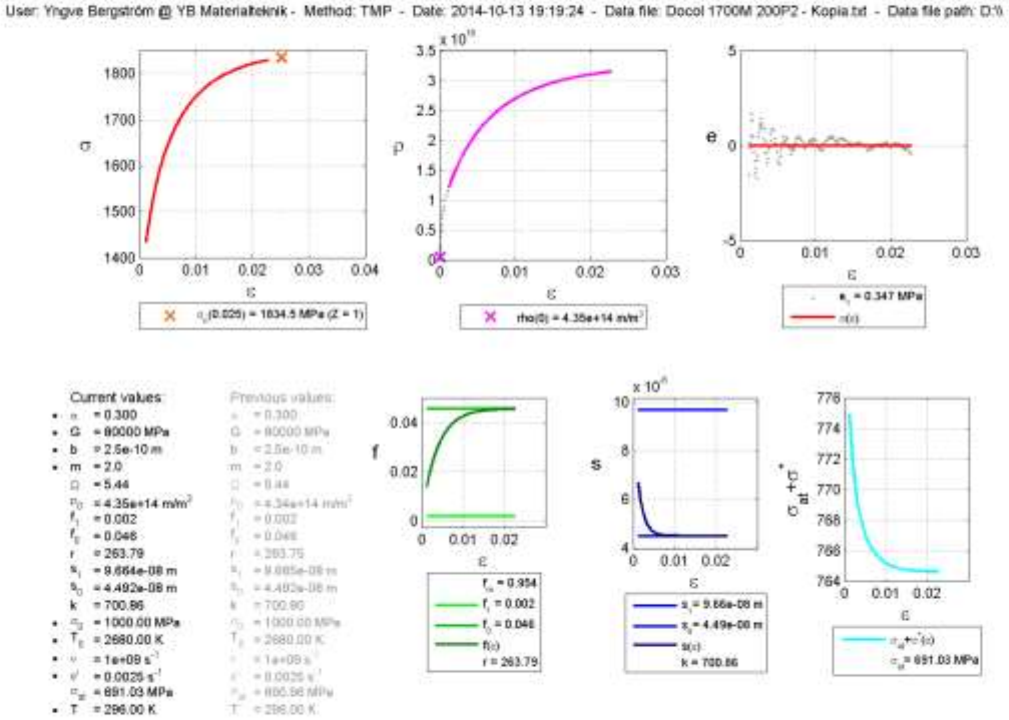

User: Yngve Bergström @ YB Materialteknik - Method: TMP - Date: 2014-10-13 19:19:24 - Data file: Docol 1700M 200P2 - Kopia.txt - Data file path: D:\

Current values:
• $\alpha$ = 0.300
• G = 80000 MPa
• b = 2.5e-10 m
• m = 2.0
$\Omega$ = 5.44
$\rho_0$ = 4.35e+14 m/m$^2$
$f_i$ = 0.002
$f_0$ = 0.046
r = 263.79
$s_i$ = 9.664e-08 m
$s_0$ = 4.492e-08 m
k = 700.86
• $\sigma_0$ = 1000.00 MPa
• $T_E$ = 2680.00 K
• $\nu$ = 1e+09 s$^{-1}$
• $\dot{\varepsilon}$ = 0.0025 s$^{-1}$
$\sigma_{ai}$ = 891.03 MPa
• T = 296.00 K

Previous values:
$\alpha$ = 0.300
G = 80000 MPa
b = 2.5e-10 m
m = 2.0
$\Omega$ = 5.44
$\rho_0$ = 4.34e+14 m/m$^2$
$f_i$ = 0.002
$f_0$ = 0.046
r = 263.75
$s_i$ = 9.665e-08 m
$s_0$ = 4.492e-08 m
k = 700.90
$\sigma_0$ = 1000.00 MPa
$T_E$ = 2680.00 K
$\nu$ = 1e+09 s$^{-1}$
$\dot{\varepsilon}$ = 0.0025 s$^{-1}$
$\sigma_{ai}$ = 890.96 MPa
T = 296.00 K

*Fig.11b Fitting of inhomogeneity theory to Martensitic 1700M steel - for compilation of all parameter values, Table 6*

Below the results from fitting the theory to the remaining metals are presented, see also Table 6.

## A4 – SOFT FERRITE

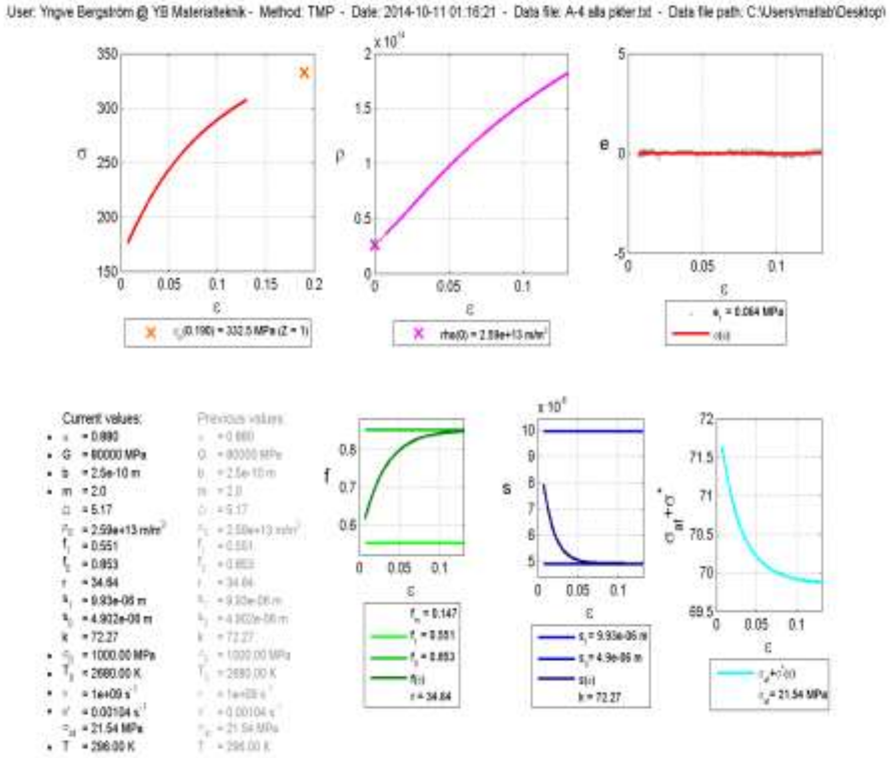

User: Yngve Bergström @ YB Materialteknik - Method: TMP - Date: 2014-10-11 01:16:21 - Data file: A-4 alla plder.txt - Data file path: C:\Users\matlab\Desktop\

Current values:
• $\alpha$ = 0.880
• G = 80000 MPa
• b = 2.5e-10 m
• m = 2.0
$\Omega$ = 5.17
$\rho_0$ = 2.59e+13 m/m$^2$
$f_i$ = 0.551
$f_0$ = 0.853
r = 34.84
$s_i$ = 9.93e-06 m
$s_0$ = 4.902e-06 m
k = 72.27
• $\sigma_0$ = 1000.00 MPa
• $T_E$ = 2680.00 K
• $\nu$ = 1e+09 s$^{-1}$
• $\dot{\varepsilon}$ = 0.00104 s$^{-1}$
$\sigma_{ai}$ = 21.54 MPa
• T = 296.00 K

Previous values:
$\alpha$ = 0.880
G = 80000 MPa
b = 2.5e-10 m
m = 2.0
$\Omega$ = 5.17
$\rho_0$ = 2.59e+13 m/m$^2$
$f_i$ = 0.551
$f_0$ = 0.853
r = 34.84
$s_i$ = 9.93e-06 m
$s_0$ = 4.902e-06 m
k = 72.27
$\sigma_0$ = 1000.00 MPa
$T_E$ = 2680.00 K
$\nu$ = 1e+09 s$^{-1}$
$\dot{\varepsilon}$ = 0.00104 s$^{-1}$
$\sigma_{ai}$ = 21.54 MPa
T = 296.00 K

*Fig. 11c Fitting of inhomogeneous theory to A4 soft ferrite, for a compilation of parameter values - Table 6*

## AA3003 – PARTICLE STRENGTHENED ALUMINUM

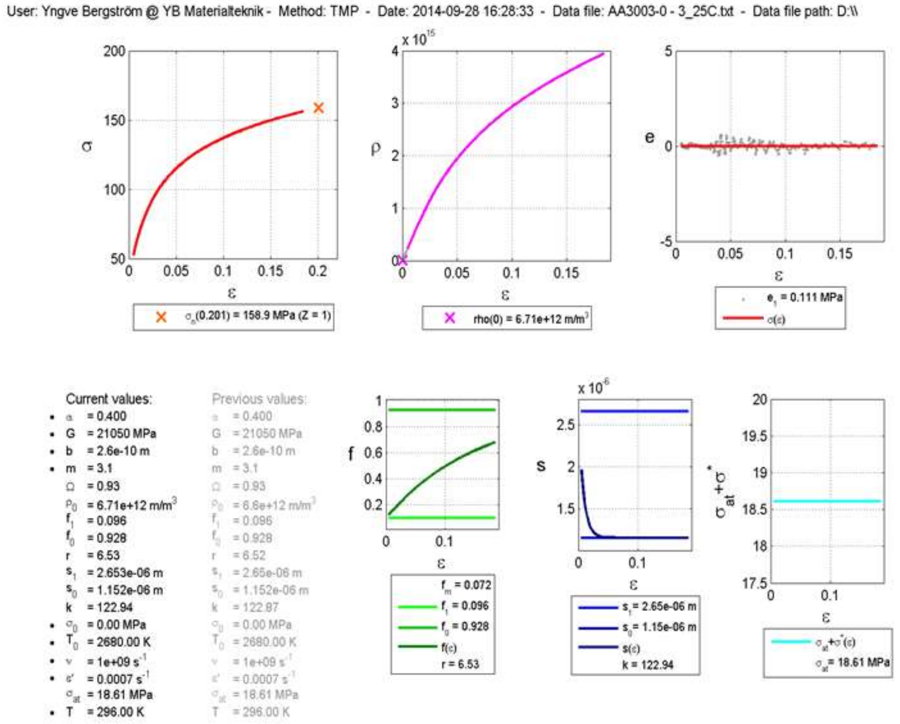

| Current values: | Previous values: |
|---|---|
| • α = 0.400 | α = 0.400 |
| • G = 21050 MPa | G = 21050 MPa |
| • b = 2.6e-10 m | b = 2.6e-10 m |
| • m = 3.1 | m = 3.1 |
| Ω = 0.93 | Ω = 0.93 |
| $\rho_0$ = 6.71e+12 $m/m^3$ | $\rho_0$ = 6.6e+12 $m/m^3$ |
| $f_1$ = 0.096 | $f_1$ = 0.096 |
| $f_0$ = 0.928 | $f_0$ = 0.928 |
| r = 6.53 | r = 6.52 |
| $s_1$ = 2.653e-06 m | $s_1$ = 2.65e-06 m |
| $s_0$ = 1.152e-06 m | $s_0$ = 1.152e-06 m |
| k = 122.94 | k = 122.87 |
| • $\sigma_0$ = 0.00 MPa | $\sigma_0$ = 0.00 MPa |
| • $T_0$ = 2680.00 K | $T_0$ = 2680.00 K |
| • ν = 1e+09 $s^{-1}$ | ν = 1e+09 $s^{-1}$ |
| • ε' = 0.0007 $s^{-1}$ | ε' = 0.0007 $s^{-1}$ |
| $\sigma_{at}$ = 18.61 MPa | $\sigma_{at}$ = 18.61 MPa |
| • T = 296.00 K | T = 296.00 K |

*Fig. 11c Fitting inhomogeneous theory to AA3003 – for compilation of all parameter values, Table 6*

## Al+0.052% Ti

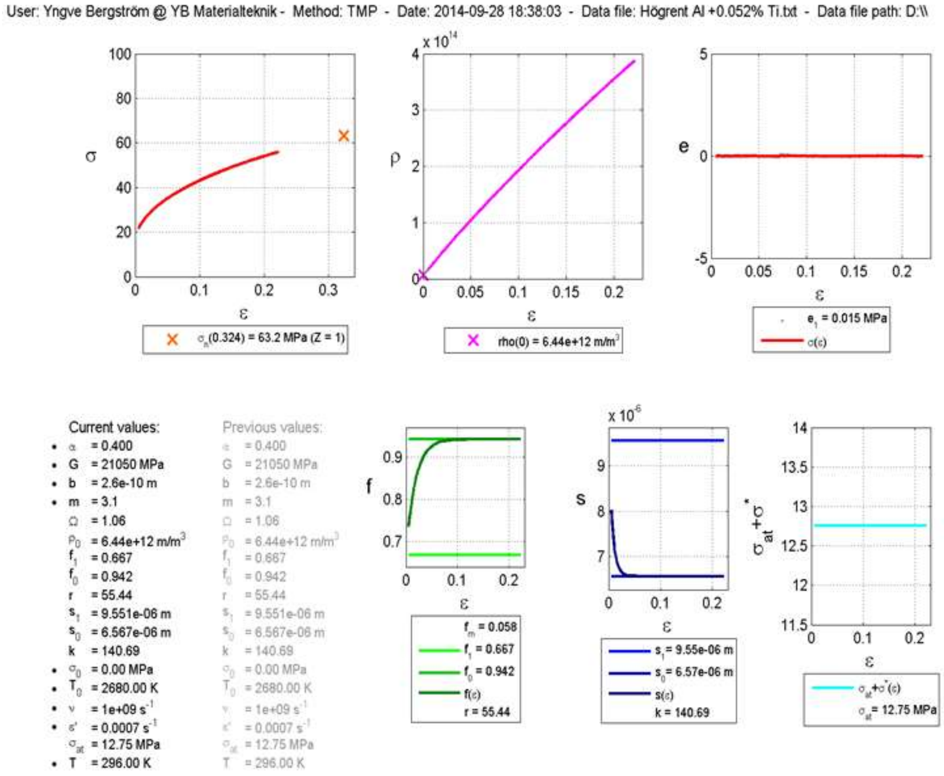

| Current values: | Previous values: |
|---|---|
| • α = 0.400 | α = 0.400 |
| • G = 21050 MPa | G = 21050 MPa |
| • b = 2.6e-10 m | b = 2.6e-10 m |
| • m = 3.1 | m = 3.1 |
| Ω = 1.06 | Ω = 1.06 |
| $\rho_0$ = 6.44e+12 $m/m^3$ | $\rho_0$ = 6.44e+12 $m/m^3$ |
| $f_1$ = 0.667 | $f_1$ = 0.667 |
| $f_0$ = 0.942 | $f_0$ = 0.942 |
| r = 55.44 | r = 55.44 |
| $s_1$ = 9.551e-06 m | $s_1$ = 9.551e-06 m |
| $s_0$ = 6.567e-06 m | $s_0$ = 6.567e-06 m |
| k = 140.69 | k = 140.69 |
| • $\sigma_0$ = 0.00 MPa | $\sigma_0$ = 0.00 MPa |
| • $T_0$ = 2680.00 K | $T_0$ = 2680.00 K |
| • ν = 1e+09 $s^{-1}$ | ν = 1e+09 $s^{-1}$ |
| • ε' = 0.0007 $s^{-1}$ | ε' = 0.0007 $s^{-1}$ |
| $\sigma_{at}$ = 12.75 MPa | $\sigma_{at}$ = 12.75 MPa |
| • T = 296.00 K | T = 296.00 K |

*Fig. 11c Fitting inhomogeneous theory to Al+0.052% Ti - for a compilation of all parameter values, Table 6*

## STAINLESS AUSTENITIC STEEL

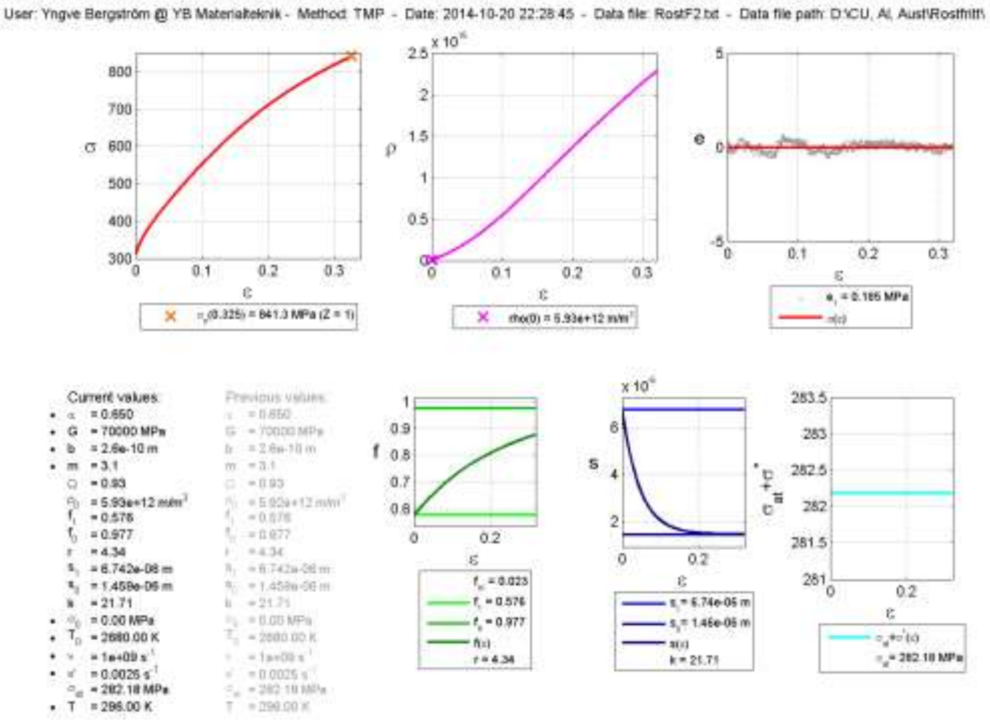

User: Yngve Bergström @ YB Materialteknik - Method: TMP - Date: 2014-10-20 22:28:45 - Data file: RostF2.txt - Data file path: D:\CU, Al, Aust\Rostfritt\

Current values:

- α = 0.650
- G = 70000 MPa
- b = 2.6e-10 m
- m = 3.1
- Ω = 0.93
- $\rho_0$ = 5.93e+12 m/m$^3$
- $f_1$ = 0.576
- $f_0$ = 0.977
- r = 4.34
- $s_1$ = 6.742e-06 m
- $s_0$ = 1.459e-06 m
- k = 21.71
- $\sigma_0$ = 0.00 MPa
- $T_0$ = 2680.00 K
- ν = 1e+09 s$^{-1}$
- $\dot{\varepsilon}$ = 0.0025 s$^{-1}$
- $\sigma_{at}$ = 282.18 MPa
- T = 296.00 K

Previous values:

- α = 0.650
- G = 70000 MPa
- b = 2.6e-10 m
- m = 3.1
- Ω = 0.93
- $\rho_0$ = 5.93e+12 m/m$^3$
- $f_1$ = 0.576
- $f_0$ = 0.977
- r = 4.34
- $s_1$ = 6.742e-06 m
- $s_0$ = 1.459e-06 m
- k = 21.71
- $\sigma_0$ = 0.00 MPa
- $T_0$ = 2680.00 K
- ν = 1e+09 s$^{-1}$
- $\dot{\varepsilon}$ = 0.0025 s$^{-1}$
- $\sigma_{at}$ = 282.18 MPa
- T = 296.00 K

*Fig. 11c. Fitting inhomogeneous theory to stainless austenitic steel, for a compilation of all parameter values, Table6*

### Table 6: Compilation of parameter values from Fig. 11, 12 and 13

| ***Parameter*** | ***1700M*** | ***DP 800*** | ***AA3003*** | ***A4 – ferrit*** | ***Al – 0.052Ti*** | ***Rostfritt*** |
|---|---|---|---|---|---|---|
| **α** | 0,3 | 0,5 | 0,4 | 0,88 | 0,4 | 0,65 |
| **MPa** | 80000 | 80000 | 21050 | 80000 | 21050 | 70000 |
| **b m** | 2,5E-10 | 2,5E-10 | 2,6E-10 | 2,5E-10 | 2,6E-10 | 2,6e-10 |
| **m** | 2 | 2 | 3,1 | 2 | 3,1 | 3,1 |
| **Ω** | 5,44 | 5,02 | 0,93 | 5,17 | 1,06 | 0,93 |
| **ρ0, m/m3** | 4,35E14 | 1,42E14 | 6,71E12 | 2,59E13 | 6,44E12 | 5,93e12 |
| **f1** | 0,002 | 0,152 | 0,096 | 0,551 | 0,667 | 0,576 |
| **f0** | 0,046 | 0,727 | 0,928 | 0,853 | 0,942 | 0,977 |
| **r** | 263,79 | 20,66 | 6,53 | 34,64 | 55,44 | 4,34 |
| **S1, m** | 9,664E-8 | 7,584E-7 | 2,653E-6 | 9,93E-6 | 9,551E-6 | 6,74e-6 |
| **S0, m** | 4,492E-8 | 5,178E-7 | 1,152E-6 | 4,902E-6 | 6,567E-6 | 1,46e-6 |
| **k** | 700,86 | 305,4 | 122,94 | 72,27 | 140,69 | 21,71 |
| **σ0, MPa** | 1000 | 1000 | 0 | 1000 | 0 | 0 |
| **T0, K** | 2680 | 2680 | 2680 | 2680 | 2680 | 2680 |
| **ν, s-1** | 1E9 | 1E9 | 1E9 | 1E9 | 1E9 | 1E9 |
| **$\dot{\varepsilon}$ , s-1** | 0,0025 | 0,0104 | 0,0007 | 0,00104 | 0,0007 | 0,0025 |
| **σat, MPa** | 691,03 | 434 | 18,61 | 21,54 | 12,75 | 282,18 |
| **T, K** | 296 | 296 | 296 | 296 | 296 | 296 |

## COMMENTS TO THE FITTING RESULTS

- In general we can conclude that of the various parameters involved in the theory, the following 9 are constants with known values: α, G, b, m, $\sigma_0$, $T_0$, ν, $\dot{\varepsilon}$ and T. They represent tabulated data and experimentally determined parameters such as temperature, T, and applied strain rate $\dot{\varepsilon}$ .

- The following parameters have been allowed to vary: Ω, $\rho_0$, $f_1$, $f_0$, r, $s_1$, $s_0$, k and $\sigma_{at}$. Here it holds that $f_0 = 1 - f_h$ , where $f_h$ is the hard phase, for instance martensite in DP steel. Since the martensite content can be experimentally measured the value of $f_0$ is also known. In ferrite Ω~5 at room temperature and normal strain rates. For ferrite based steels it therefore holds that the number of variable parameters is ~ 7. The parameters $s_1$, $s_0$ and $\rho_0$ can be estimated using e.g. TEM – analysis and the number of uncertain parameter values are then down to 4.
- *In the case of DP steels, however, most of the above mentioned parameter values can be estimated from the current martensite content with surprisingly good accuracy, why the number of varying parameters for this type of material, can be limited to 1 or 2. These results are currently being processed and will be featured in an upcoming article.*
- In the above fitting procedure all parameters have been allowed to vary freely, even for the DP800 steel.
- We assume that the best fit is achieved when $e_1$ exhibits a minimum. There can be multiple minima, and it is therefore important to find the right adjustment which is assumed to be the one with the smallest error.
- The statistical error e1 is normally greater in markedly inhomogeneous materials. We can, for example, compare materials 1700M with e1= 0.347 MPa and the single-phase ferritic steel A-4 with e1= 0.064 MPa. An important explanation for this behavior is that 1700M is full of residual stresses and stress concentrations while the A-4 is not. We also see that $e_1$ reduces with increasing strain in the martensitic steel, which is not the case for A-4. This latter effect presumably depends on the release of residual stresses in the 1700M. A comparison of AA3003 and Al 0.052Ti shows a similar behavior. In the single-phase materials, this effect is marginal.
- The fact that the remobilization constant, Ω, assumes a value around 5 at the prevailing experimental conditions – RT and a moderate applied strain rate – shows that the plastic deformation is localized to the ferrite in the three steels DP800, 1700M and A-4. In the cases of AA3003 and Al 0.052Ti the deformation process is localized to aluminum with a Ω - value around 1. The low values of the remobilization constant in the latter two materials are inter alia due to the fcc-structure of these metals. Small Ω-values result in a high strain hardening and thus a better ductility.
- The martensitic steel 1700M has the highest grown-in dislocation density, $\rho_0$ = 4.35E14 $m^{-2}$ and DP800 has the second highest value $\rho_0$ = 1.43E14. Since the martensitic material has a very high martensite concentration, about 96%, compared with about 25% of the DP800 steel, the plastic deformation occurring as a result of the austenite/martensite transformation becomes significantly larger. The single-phase materials exhibit consistently lower $\rho_0$-values.
- $f_1$ indicates the value of the average volume fraction initially participating in the plastic deformation process. $f_0$ indicates the total available volume fraction. For the DP800 steel it holds that approximately 14.8% of the total volume fraction is initially involved. The active volume fraction then grows with increasing strain towards a value of 74.5%. The latter result suggests that the volume fraction of hard martensite is (100%-74.5%=24.5%). In the case of the martensitic steel 1700M the corresponding values are 0.2% and 4.4%. These latter, extremely small values, give rise to a very powerful rate of strain hardening, which, according to what the structural analysis suggests, is located in a thin layer, in close contact with the old austenitic grain boundaries. The volume fraction of martensite in the 1700M steel is then approximately 95.6%.
- In the case of AA3003 containing a volume fraction of hard, coarse particles, an active volume fraction of about 9.5% is involved in the initial stage of the deformation process. In the final

phase of deformation around 93% of the specimen is engaged. This suggests that the volume fraction of active particles is about (100% - 93%) = 7% which agrees well with experiments.

- $s_1$ specifies how far, on average, mobile dislocations initially move and $s_0$ how far, on average, they move at larger strains. In the case of the 1700M steel $s_1$ ~ 9.9E-8 m and at the end of straining it moves around $s_0$ ~ 4.5E-8 m. The distance the dislocations move is thus at the nano - level in the martensitic steel. The corresponding distances for the pure ferritic steel A-4 are 9.9E-6 m and 4.9E-6 m, i.e. micro level. These small s-values therefore, together with the small f-values, contribute to the high rate of strain hardening of this martensitic steel. The much higher s- and f-values for the A-4 steel result in a much smaller rate of strain hardening.
- In the case of the athermal friction stress, $\sigma_{at}$, it is greatest for the 1700M – steel with a value of 701.86 MPa, the second largest of the DP800-steel with a value of 432.03 MPa. The pure ferritic steel has the value 21.54 MPa.
- AA3003 has a $\sigma_{at}$ – value of 18.61 MPa and Al-0.052%Ti a value of 12.75 MPa.
- The thermal component, $\sigma^*$ ($\varepsilon$), varies with strain rate and temperature in ferritic materials. In connection with inhomogeneous plastic deformation the active volume fraction, f($\varepsilon$), increases from a low $f_1$ – value to a larger $f_0$ – value. This means that the local strain rate decreases from a high to a low value. In the case of the 1700M - steel the total friction stress $\sigma_{i0} = \sigma_{at} + \sigma^* =$ 776 MPa, see Table 6. The athermal stress $\sigma_{at}$ = 691 MPa. The maximum thermal friction stress is therefore equal to 85 MPa. With increasing strain up to necking the thermal stress decreases to 73 MPa. The thermal stress has therefore decreased by 12 MPa during straining. By taking this into account we have slightly improved the accuracy of fit. The steels DP800 and A-4 exhibit a similar behavior. In the case of fcc-materials the thermal stress can be neglected.
- How large are the local strains in the above studied materials in comparison to the global ones? We will deal with that in the upcoming section.

## GLOBAL AND LOCAL STRAINS DURING UNIAXIAL STRAINING

### Multi – phase materials:

The inhomogeneity of metallic materials leads to a localization of the plastic deformation process, to an active average volume fraction, f($\varepsilon$), of the test sample. This means that the local strains will be greater than the global ones determined from standard uniaxial tensile testing, see eq. (16). We have in the present investigation studied various materials with different types of inhomogenities and we will now compare these effects exhibited by the following materials: 1700M, DP800 and AA3003 containing different amounts and types of soft and hard phases. We will also investigate the single-phase materials, namely the ferritic steel A-4, the high purity Al+0.052%Ti material and an austenitic stainless steel, see Table 6.

#### Martensitic (low carbon) steel – 1700M

1700M has a basic structure of low temperature-tempered martensite (200C) and for the soft active volume fraction, see Table 6, it holds that $f_1$ ~ 0.2% and $f_0$ ~ 5%. These extremely low volume fractions have a powerful effect on the work hardening - see Fig. 14 - where the true stress is plotted versus the global strain, red curve, as well as versus the local strain, blue curve. We can see that the localization leads to an extremely high local rate of work hardening with the positive effect that the steel withstands a global strain of 2% giving rise to a true flow stress of 1800 MPa. The corresponding local strain is, in fact, close to 55%.

By minimizing the active volume fraction, the materials hardness and ductility are maximized.

At the same time we also know which physical mechanisms it is that give rise to these valuable properties, namely the following:

- Large $\rho_0$ values emanating from the martensite transformation, 4.35E14 $m^{-2}$ give rise to high yield points and tensile strengths as well as small dislocation cell diameters. This in turn leads to a diminishing mean free path of dislocation motion and a high rate of strain hardening.
- Small f-values, see above , automatically increases the rate of strain hardening
- The production process behind this martensitic steel is such that the ratio of the crystal axis c and a, i.e. c/a ~ 1. Hence, the crystal structure is bcc with the result that the quantity of carbon in solution is very small. We may therefore assume that the carbon solution hardening effect is small. This is both positive (small strain ageing effects) and negative (lower yield and fracture stresses).
- Small s-values ($s_1$ = 9.93E-8 m and $s_0$ = 4.9E-8 m) - increase in the rate of strain hardening
- Large athermal friction stress (691.03 MPa) leads to high yield and fracture stresses.
- There are good reasons to believe that the high athermal friction stress value emanates from small carbon based particles which are formed during the hardening procedure. If we assume that the average distance between these particles is, λ, then from a simple particle hardening relationship we have that

$$\lambda = \frac{m \cdot G \cdot b}{\sigma_{at}}$$

- With m = 2, G = 80000 MPa, b = 2.5E-10 m and σat = 691 MPa we have that λ ~ 5.8E-8 m. Since this value lies between the s1 – and s2 – values, see Table 6, there are good reasons to believe that it is the particle hardening that mainly controls the value of σat.

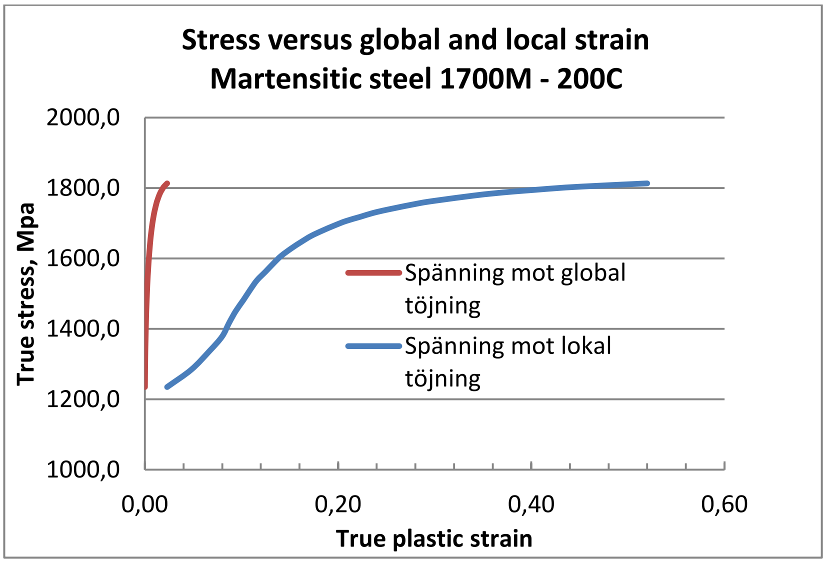

*Fig.14. True stress versus global (red curve) and local (blue curve) true strain*

### DP 800

The corresponding result for the DP 800 steel is shown in Fig. 15. In this case a global strain of about 6% leads to an average local strain of around 11%.

One basic reason for these lower values, as compared to the martensitic steel 1700M, is that the active local volume fraction soft phase (ferrite) is considerable larger ($f_1$ =0.152 and $f_0$ = 0.727) and that the mean free path of mobile dislocation motion, s is larger ($s_1$ = 7.58E-7 m and $s_0$ = 5.18E-7 m), see Table 6.

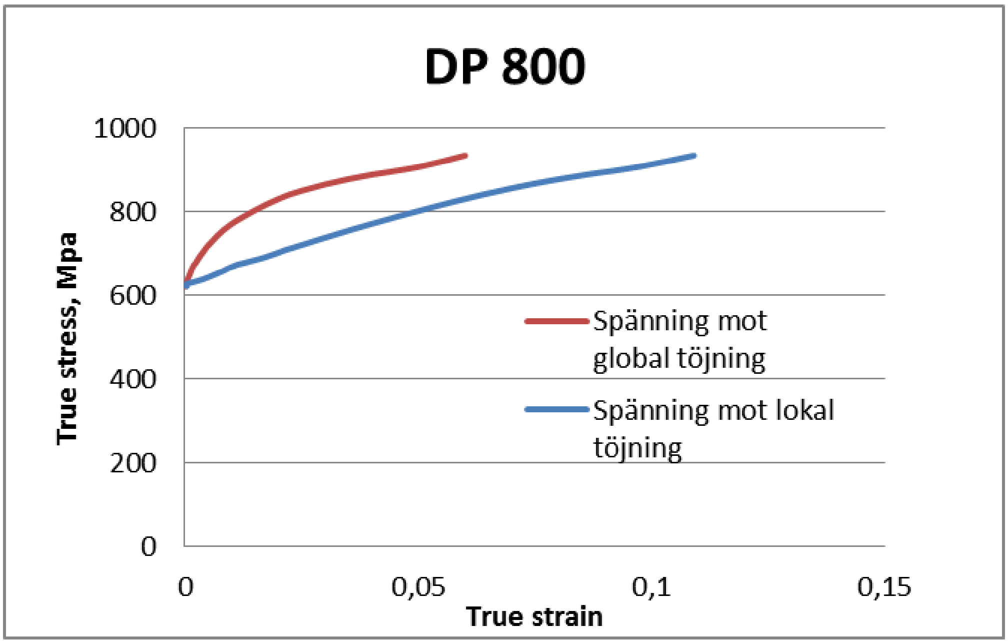

*Fig 15.True plastic strain versus global strain (red curve) and local strain (red curve)*

It also holds that the athermal friction stress $\sigma_{at}$ = 434 MPa is considerable lower than that of the martensitic steel 1700M. Likewise it holds that the grown-in dislocation density, $\rho_0$, 1.42E14 m for DP800 compared with 4.35E14 for 1700M. The positive effects, however, are tangible and give DP800-steel reasonable high values in terms of strength and ductility.

### AA3003

It is interesting to note that the Al-based material AA 3003, containing hard particles with an average diameter of about 10 µm, exhibits effects similar to those observed in steels 1700M and DP 800, see Fig 16. The ductility of the material is good which depends on the low value of **Ω** ~ 1 and the low strength.

The low strength of the material is of course a drawback and depends on the following factors – see Table 6:

- large $f_1$ – and $f_2$ – values
- large $s_1$ - and $s_2$ – values
- small $\rho_0$ – values
- small $\sigma_{at}$ – values

(In the present Al – case the global strain to necking is ~ 16% while the corresponding local strain is about 26%).

One possible way of improving the strength of this type of materials would be to add into the material small-sized particles to increase its particle-hardening effect.

By controlling the average size and the distance between these particles, this would also result in a decrease of the $s_1$- and $s_0$ – values and hence an increase the rate of strain hardening.

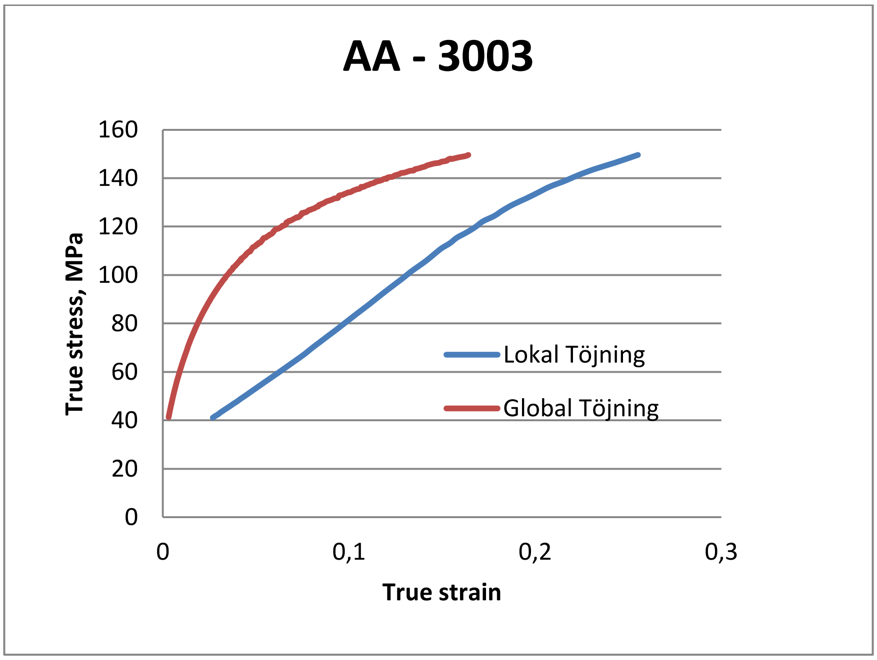

*Fig.16. True stress versus global strain (red curve) and local strain (blue curve)*

## Single-phase materials:

### Ferritic steel – A4

An example of inhomogeneity in single-phase metals is what we observe in the soft ferritic steel A4, see Fig. 17. After ca ~1% of global strain the local strain is ~1.2%, i.e. a difference of 0.2%. After ~13% of global strain the local strain attains a value of ~15%, i.e. a difference of 2%. What we can see here are relatively small effects of inhomogeneity but there is, never the less, clear inhomogeneous tendencies. A possible explanation for the inhomogeneity is variations in texture, grain diameter and the presence of small residual stresses. The low work hardening rate is due partly to high $f_1$ and $f_0$ values, large $s_1$ and $s_0$ values and a high Ω-value. The lower strength can be referred to a low $\rho_0$ –value and a lower friction stress, $\sigma_{at}$.

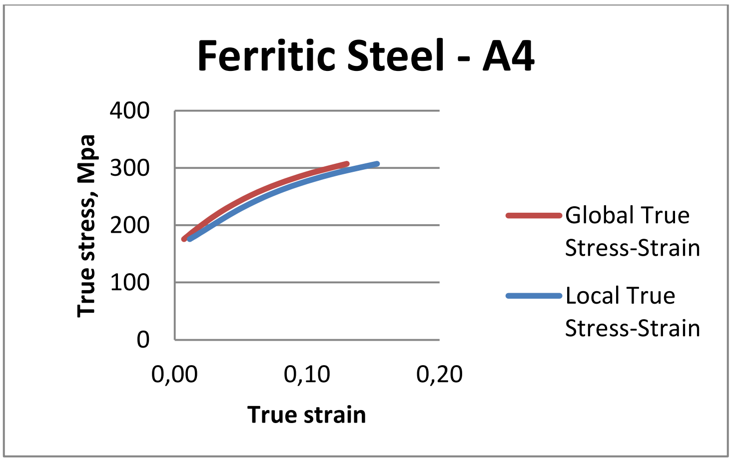

*Fig 17 True stress versus true global strain (red curve) and true local strain (blue curve)*

### Austenitic stainless steel

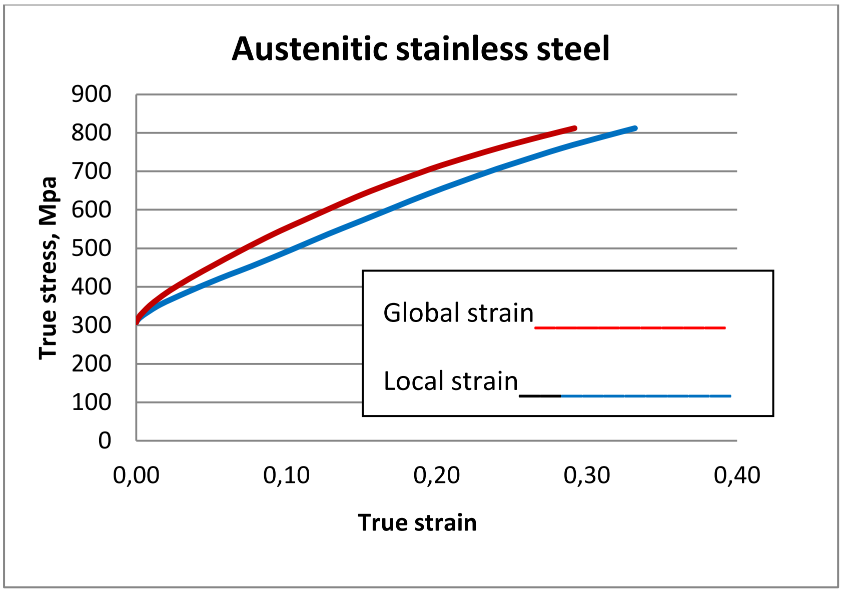

*Fig. 18 True stress versus global strain (red curve) and local strain (blue curve)*

An example of a slight inhomogeneity in commercial stainless austenitic steel is shown in Fig. 18. In this case it holds that the global strain to necking is ca 29% (red curve) while the corresponding local strain is 33% (blue curve). The inhomogeneous effect is, however, somewhat stronger than that in the ferrite steel, see Fig. 17, but much smaller than in DP 800, 1700M and AA3003. There might be effects of some type of second phases or twinning.

### Highpure Al+0.052Ti

The pure Al + 0.052%Ti material appears to be least affected by inhomogeneous plastic deformation. This is of course related to the high cleaness of the material. The local strain is, however, 1.5 % greater than the global after straining up to necking.

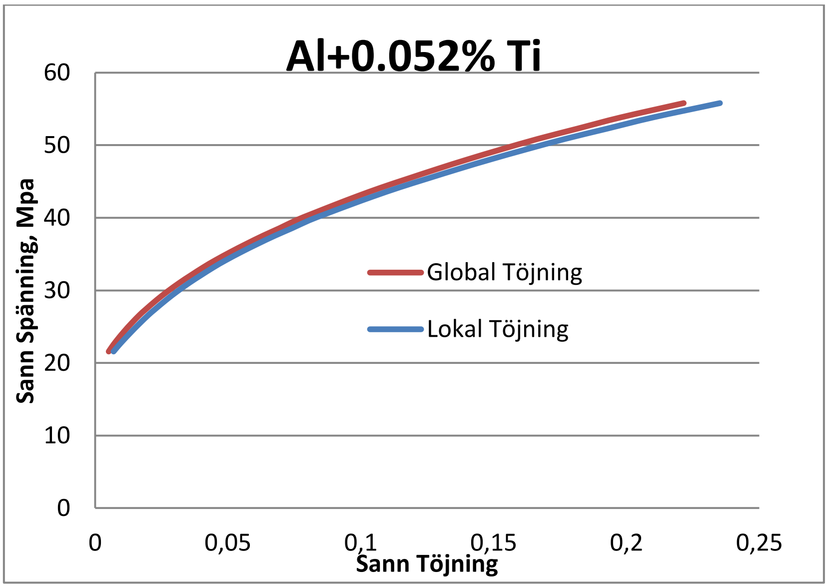

*Fig. 19. True stress versus global strain (red curve) and local strain (blue curve)*

## COMPARISON BETWEEN SINGLE-PHASE AND MULTI-PHASE MATERIALS

We have analyzed three multiphase materials, namely, 1700M, DP800 and AA3003 and three single-phase materials, namely a soft ferritic steel A4, an austenitic stainless steel and a high purity Al-material Al+0.052%Ti with respect to the inhomogeneity.

The results of the present study clearly show that a mixture of hard and soft phases gives rise to a localization of the plastic deformation process to the softer phases. The higher the volume fraction of hard phase, the less soft phase and the more powerful the strain hardening, see Fig 14 -16.

Also the single-phase materials show an inhomogeneous behavior, but significantly weaker. In the former case it is the larger volume fractions of hard phases and the plastically active volume fractions, which control the inhomogeneous effect. In the latter case inhomogeneity is caused by weaker factors like varying directions among the grains, texture, varying small-particle size and distribution, residual stresses, etc.

The Al+0.052%Ti material exhibited the smallest inhomogeneity effect.

The analysis suggests, therefore, that pure single-phase metals, should normally give acceptably good results by applying theories which are not corrected for inhomogeneity.

To achieve reliable results in analyzing multi-phase materials, corrections must be carried out. If this is not done the results will be difficult to interpret.

## WHAT CAN VI DO TO FURTHER IMPROVE THE PROPERTIES OF INHOMOGENEIOUS METALS

This study clearly shows that it is the macroscopic inhomogeneity which is the cause of the excellent strength- and ductility properties of modern high strength materials as DP – steels, low-temperature tempered martensitic steel and coarse particle hardened single-phase materials.

Steel is a unique material since it is possible by varying chemical compositions and process routines to obtain a variety of combinations of hard phases such as pearlite, bainit and martensite with the soft phase ferrite.

One can also utilize hard particles of different size and high melting temperature to achieve even better properties.

Another example is the possibility to improve the strength and ductility of soft fcc-metals like e.g. Al and Cu by addition of hard particles of varying sizes.

We have already shown how the strength and ductility of a soft Al – phase can be improved by addition of 10 µm size hard particles and why this occurs.

The present theory is obviously well suited to analyze, in some detail, various types of high strength metals consisting of various combinations of hard and soft phases.

In an ongoing study a detailed analysis is carried out on DP-steels containing varying amounts of martensite. The hope is to achieve new knowledge of how to further improve these materials strength and ductility. It has also been observed that there is a close correlation between the values of the parameters involved in the theory and the martensite content. This will make the fitting process safer and increases the possibility to improve the properties of this type of material.

Another hope is that, as in the case for DP-steel, it will be possible to find simple relationships between the parameter values of the theory and for example the martensite content or the volume fraction of the soft phase. It would also be of great interest to in more detail study particle hardening process in various fcc metals like aluminum and copper, for instance.

## RESULTS AND CONCLUSIONS

- In the present paper we start by presenting a summary of the development, which Bergströms dislocation theory for the plastic deformation of metallic materials has undergone over the past 50 years: Stages I – III. All steps are based on the assumption that Taylors equation for the relationship between a materials true stress, $\sigma$ ($\varepsilon$), and total dislocation density, $\sqrt{\rho}$, apply. The theory holds for uniaxial straining up to necking where strain is the true strain.
- Stage I is mainly focused on pure, homogeneous, single-phase materials and shows how, by starting from the laws of natural growth and natural decay, it is possible to describe how immobilized dislocations re-mobilize proportional to the rate constant, **$\Omega$**, and that the mobile dislocations mean free path, $s(\varepsilon)$, is strain independent and equal to $s_0$.
- In Stage II it is still assumed that the material is homogeneous and that the mean free path of dislocation motion, $s(\varepsilon)$, decreases with strain from an initial value, $s_1$, to a final value, $s_0$, according to natural decay, where k is the rate constant.
- The final development step, Step III, is new and includes the macroscopically inhomogeneous plastic deformation of materials containing a mixture of hard and soft phases of the type observed in DP steels, low temperature annealed martensitic steels of fairly low carbon content like 1700M. Also material AA3003 consisting of a soft Al-phase and hard particles of size ~ 10 µm is inhomogeneous and exhibits a work-hardening behavior similar to the two above mentioned steels.
- Structural studies of uniaxial tensile test specimens show that the plastic deformation process is located to an active volume fraction, $f(\varepsilon)$, of the specimen volume. The greater the fraction of hard phase, the greater the rate of strain hardening and the greater the strength.
- Even pure single-phase soft metals such as ferrite and aluminum exhibit a certain inhomogeneous behavior since all materials contain inhomogenities, such as texture, varying grain diameters, varying slip plane directions, residual stresses, etc. This type of inhomogeneity effect is small and can usually be neglected.
- Bergströms original theory has now been upgraded in such a way that it takes into account the strain dependent, localized volume fraction, $f(\varepsilon)$, which characterizes the plastic deformation process of inhomogeneous materials of the above mentioned type. This allows the stress to be determined as a function of both the global and the local strains. It turns out, for example that the global strain to necking of the martensitic steel 1700M is about 2%, while the corresponding local average strain is about 55%.
- The analysis of the uniaxial stress-strain behavior makes it possible to determine the value of the initial active volume fraction, $f_1$, and the final active volume fraction, $f_0$.
- Also the initial, $s_1$, and final, $s_0$, mean free paths of mobile dislocations can be determined as well as the athermal, $\sigma_{at}$, the thermal, $\sigma^*$, friction stresses. Also the grown-in dislocation density, $\rho_0$, can be estimated.
- This makes it possible to see how the individual parameters vary with chemical composition, structure, volume fractions of hard and soft phases, process parameters etc. Starting from this basic knowledge will help us to develop the right material properties for different applications.

## THANK YOU FOR YOUR HELP

To Joachim Larsson, SSAB, and Hans - Erik Ekström, SAPA GROUP:

Heartfelt thanks for valuable discussions related to the plastic deformation process of homogeneous and inhomogeneous metals.

# REFERENCES

(1) C. Federici, S.Maggi, and S. Rigoni. The Use of Advanced High Strength Steel Sheets in the Automotive Industry, Fiat Auto -Engineering & Design, Turin, Italy, 2005

(2) J. R. Fekete, J. N. Hall, D. J. Meuleman, and M. Rupp,"Progress in implementation of advanced high-strength steelsinto vehicle structures," Iron & Steel Technology, vol. 5, no. 10, pp. 55–64, 2008

(3) R. Koehr, ULSAB-AVC Advanced Vehicle Concepts Overview Report, in Safe, Affordable, Fuel Efficient Vehicle Concepts for the 21st Century Designed in Steel, Porsche Engineering Services, Detroit, Mich, USA, 2002.

(4) P. Tsipouridis, E. Werner, C. Krempaszky, and E. Tragl,"Formability of high strength dual-phase steels," Steel Research International, vol. 77, no. 9-10, pp. 654–667, 2006

(5) M. Takahashi, "Development of high strength steels for automobiles," Nippon Steel Technical Report, no. 88, pp. 2–7, 2003

(6) J. Bouquerel, K. Verbeken, and B. C. De Cooman, "Microstructure-based model for the static mechanical behavior of multiphase steels," Acta Materialia, vol. 54, no. 6, pp. 1443–1456, 2006

(7) V. Colla, M. De Sanctis,A. Dimatteo,G. Lovicu, A. Solina, and R. Valentini, "Strain hardening behavior of dual-phase steels," Metallurgical and Materials Transactions A, vol. 40, no. 11, pp 2557–2567, 2009

[8] Z. H. Cong, N. Jia, X. Sun, Y. Ren, J. Almer, and Y. D. Wang,"Stress and strain partitioning of ferrite and martensite during deformation," Metallurgical and Materials Transactions A, vol. 40, no. 6, pp. 1383–1387, 2009

(9) Z. Jiang, Z. Guan, and J. Lian, "Effects of microstructure variables on the deformation behavior of dual-phase steel,"Materials Science and Engineering A, vol. 190, no. 1-2, pp. 55–64, 1995.

(10) C. Kim, "Modeling tensile deformation of dual-phase steel. "Metallurgical Transactions A, vol. 19, no. 5, pp. 1263–1268,1988.

(11) M. F. Ashby, "The deformation of plastically nonhomogeneous alloys," in Strengthening Method in Crystals, A. Kelly and B. Nicholson, Eds., Applied Science Publishers LTD, London, UK, 1971.

(12) H. Mughrabi, "Dual role of deformation -induced geometrically necessary dislocations with respect to lattice plane misorientations and/or long-range internal stresses," Acta Materialia, vol. 54, no. 13, pp. 3417–3427, 2006(13).

(13) Y. Bergström, Y. Granbom and D. Sterkenburg, "A dislocation-based theory for the deformation hardening behavior of DP steels: Impact on martensite content and ferrite grain size,"Journal of Metallurgy, vol. 2010, Article ID 647198, 16 pages, 2010

(14) Y. Bergström, "The plastic deformation of metals—a dislocation model and its applicability," Reviews on Powder Metallurgy and Physical Ceramics, vol. 2, no. 2-3, pp. 79–265, 1983.

(15) G. I. Taylor, "The mechanism of plastic deformation of crystals. Part I. Theoretical," Proceedings of the Royal Society A, vol. 145, pp. 362–387, 1934

(16) D. A. Korzekwa, D. K. Matlock, and G. Krauss, "Dislocation substructure as a function of strain in a dual-phase steel, "Metallurgical Transactions A, vol. 15, no. 6, pp. 1221–1228,1984.

(17) Volterra, V., Ann. Ecole Norm. Super., 24:400, 1907

(18) I. Newton – Gravitation - Wikipedia

(19) A. Wegener – Tectonic plates – Wikipedia

(20) Y. Bergstrom - (homepage) – http://www. plastic-deformation.com

(21) Hookes lag - Wikipedia

(22) J.H. Hollomon, Trans AIME, 162, 268(1945)

(23) P. Ludwik, in: Elemente der Technologischen Mechanik, Julius Springer, Berlin, 32(1909)

# APPENDIX

## The uniaxial tensile test (homogeneous material)

The uniaxial tensile test is widely used in the metals and engineering industries and also in research and development. The procedure for determining the uniaxial tensile test curve is normally the following:

A sample with initial length, $l_0$, and initial cross-sectional area, $A_0$, is plastically deformed by a certain strain rate to an extension, Δl. Let us also assume that the applied load is, F, and that the testing volume is $V_0$.

Proceeding from such an assumption it holds that the technological strain, $\varepsilon_T$, and the technological stress, $\sigma_T$, can be written

$$\varepsilon_T = \frac{\Delta l}{l_0}$$

$$\sigma_T = \frac{F}{A_0}$$

Since the sample length and cross-sectional area continuously change during the plastic deformation process the technological strain, $\varepsilon_T$, and the technological stress, $\sigma_T$, are no truthful measures. In order to obtain the true stress, σ, we must divide the load F with the instantaneous cross sectional area, A, i.e

$$\sigma = \frac{F}{A}$$

The true strain, ε, is obtained by considering a small extension, dl, at the instantaneous length, l, and define dε as dl/l. If the test specimen has been elongated from $l_0$ to l we obtain

$$\varepsilon = \int_{l_0}^{l} \frac{dl}{l} = \ln \frac{l}{l_0}$$

Now, since $l = l_0 + \Delta l$ we obtain the following connection between the true strain, ε, and the technological strain, $\varepsilon_T$

$$\varepsilon = \ln(\frac{l_0 + \Delta l}{l_0}) = \ln(1 + \varepsilon_T)$$

In the case of homogeneous plastic deformation it is assumed that the volume, $V_0$, remains constant during straining, i.e.

$$A_0 \cdot l_0 = A \cdot l$$

The relationship between the true stress, σ, and the technological stress, $\sigma_T$, may therefore be written

$$\sigma = \frac{F}{A} = \frac{F}{A_0} \cdot \frac{A_0}{A} = \frac{F}{A_0} \cdot \frac{l}{l_0} = \sigma_T (1 + \varepsilon_T)$$

The global strain, $\varepsilon_g$, obtained in the evaluation of a uniaxial tensile stress-strain curve is according to the standard procedure based on the assumption that the total volume, $V_0$, of the specimen takes part in the deformation process and that this volume is strain independent.

Since this is normally not the case the local strain, $\varepsilon_l$,

In reality no metal is 100% homogeneous which implies that only a strain dependent fraction, $f(\varepsilon)$, of the specimen volume is active. The size of this volume depends on the degree of inhomogeneity and the speed with which this size changes with strain.

the size of this volume fraction depends on the degree of inhomogeneity and the speed with which this size changes with strain

yngve.bergstrom@gmail.com